

Bio-Systems as Super-Conductors: Part III

M. Pitkänen¹, February 1, 2006

¹ Department of Physical Sciences, High Energy Physics Division,
PL 64, FIN-00014, University of Helsinki, Finland.
matpitka@rock.helsinki.fi, <http://www.physics.helsinki.fi/~matpitka/>.
Recent address: Puutarhurinkatu 10,10960, Hanko, Finland.

Contents

1	Introduction	6
1.1	Strange behavior of cellular water and quantal ionic currents through cell membrane	7
1.2	Dark Z^0 magnetic fields and cognition	8
1.2.1	How noble gases can act as anesthetes?	8
1.2.2	Dark neutrino super conductivity	8
1.3	Atmospheric phenomena and superconductivity	9
2	Empirical support for ionic super-conductivity as a fundamental control mechanism	10
2.1	Strange behavior of the intracellular water	10
2.2	Are channels and pumps really there?	11
2.2.1	Selectivity problem	12
2.2.2	Inflation in the number of pumps and channels	13
2.2.3	Why pumping does not stop when metabolism stops?	13
2.2.4	How it is possible that ionic currents through silicon rubber membrane are similar to those through cell membrane?	14
2.3	Could the notion of the many-sheeted space-time solve the paradoxes?	14
2.3.1	Many-sheeted cell	16
2.3.2	Faraday's law of induction in the many-sheeted space-time forces electrical non-equilibrium	18
2.3.3	Flow equilibrium in many-sheeted space-time	19
2.3.4	Refinements and generalizations	21

2.3.5	Explanation of the paradoxes in terms of many-sheeted space-time	22
2.3.6	Bio-control as a control of quantum numbers characterizing supracurrents	23
2.3.7	The role of the cell membrane	24
2.4	Water memory, homeopathy, and acupuncture	25
3	Dark neutrino super conductivity	28
3.1	The analogy between superconductors of type I and quantum critical superconductors	29
3.2	Empirical guidelines	30
3.3	Dark neutrino superconductor as a quantum critical superconductor	34
3.3.1	The case of $k = 127$ neutrinos	34
3.3.2	Is neutrino superconductivity possible for $k \geq 151$?	35
3.4	Structure of brain and neutrino super conductivity	36
3.4.1	Structures in the cell length scale, miracle length scales, and twin primes	37
3.4.2	Scaled up variants of cell membrane?	38
3.4.3	Cortical structures and first level satellites of miracle length scales	38
3.4.4	Structures in the length scale of body and second level satellites of miracle length scales	40
3.5	Cognitive neutrino pairs	41
3.5.1	Cognitive neutrino pairs as $\nu\bar{\nu}$ wormhole contacts	41
3.5.2	Model for the generation of cognitive neutrino pairs	43
3.5.3	Relativistic and non-relativistic cognitive neutrino pairs	43
3.5.4	Quantization of the Z^0 magnetic flux	44
3.5.5	Does the quantum model of hearing survive the new interpretation of long ranged weak fields?	45
3.5.6	$\nu\bar{\nu}$ wormhole contacts as a source of the Z^0 magnetic field?	46
4	Atmospheric phenomena and super-conductivity	47
4.1	Tornadoes as a macroscopic quantum phenomenon involving Z^0 super-conductivity?	48
4.1.1	Tornadoes as Z^0 magnetic spiral vortices?	48
4.1.2	Tornadoes as rotating magnetic and Z^0 magnetic systems	50
4.1.3	Tornadoes as dark matter systems	51

4.2	Auroras as an astrophysical quantum phenomenon?	53
4.2.1	Basic facts, ideas and puzzles related to auroras	53
4.2.2	TGD based model for auroras	54
4.2.3	Auroras, meteors, and consciousness?	58
4.3	Lightnings, sprites, elves, and the hypothesis of magnetic sensory canvas	60
4.3.1	Lightnings	61
4.3.2	Sprites	62
4.3.3	Elves	65
4.3.4	Dark matter hierarchy, lightnings, sprites, and elves	66
4.3.5	Atmospheric electromagnetic phenomena and consciousness	68
4.3.6	What auroras, tornadoes, ball lightnings, and cold fusion might have in common?	70

Abstract

This chapter is devoted to further applications of the theory of high T_c superconductors as quantum critical superconductors involving dark matter hierarchy and large values of \hbar . The theory is applied to explain the strange findings about ionic currents through cell membrane, exotic neutrino superconductivity and the notion of cognitive neutrino pair are discussed, and the possibility that superconductivity and Bose-Einstein condensates are involved with atmospheric phenomena is considered.

1. Strange behavior of cellular water and quantal ionic currents through cell membrane

The fact that cellular water does not leak out of cell in a centrifugal force suggests that some fraction of water inside cell is in different phase. One explanation is that the nuclei of water inside cell are in doubly dark phase whereas electrons are in singly dark phase (having Compton length of 5 nm and perhaps directly "visible" using day technology!) as indeed predicted by the model of high T_c superconductivity. This conceptual framework could explain various findings challenging the notions of ionic pumps.

The empirical findings challenging the notions of ionic pumps and channels, nicely summarized by G. Pollack in his book, provide a strong support for the notions of many-sheeted space-time and ionic superconductivity.

a) The selectivity of the cell membrane implies that channels cannot be simple sieves and there must be complex information processing involved.

b) The needed number of pumps specialized to particular ions is astronomical and the first question is where to put all these channels and pumps. On the other hand, if the cell constructs the pump or channel specialized to a given molecule only when needed, how does it know what the pump looks like if it has never seen the molecule? The needed metabolic energy to achieve all the pumping and channelling is huge. Strangely enough, pumping does not stop when cell metabolism stops.

c) One can also wonder why the ionic currents through cell membrane look quantal and are same through cell membrane and silicon rubber membrane.

These observations suggest strongly the presence non-dissipative ionic currents and quantum self-organization. The TGD based explanation would be in terms of high T_c electronic and possibly even ionic superconductivity associated with cell membrane made possible by the large \hbar phase for nuclei and electrons in the interior of cell. It however seems that thermal stability conditions allow only protonic Cooper pairs in the model of ionic Cooper pairs based on direct generalization

of the model of high T_c electronic super conductivity. This does not however mean that quantal ionic currents would be absent. This empirical input also supports a view about homeostasis as a many-sheeted ionic flow equilibrium controlled by larger space-time sheets with the mediation of massless extremals (MEs) serving as space-time correlates for Bose-Einstein condensates of massless bosons (also of scaled down dark electro-weak bosons and gluons).

In the proposed picture one can understand how extremely low densities of ions and their supra currents can control much higher ion densities at the atomic space-time sheets. The liquid crystal nature of the bio-matter is crucial for the model. This vision allows also much better understanding of the effects of ELF em fields on bio-matter. Also the effects of homeopathic remedies and acupuncture known to crucially involve electromagnetic frequency signatures of chemicals can be understood if homeostasis is based on many-sheeted ionic flow equilibrium.

2. Dark Z^0 magnetic fields and cognition

Similar arguments as in the em case apply in the scale $L_w = .2 \mu\text{m}$ for Z^0 magnetic transitions with scale about 10^4 eV much above the thermal energy scale. The hierarchy of length scales is now $L_w = .2 \mu\text{m}$, $.4 \text{ mm}$, $.8 \text{ m}, \dots$ $L_w = .4 \text{ mm}$, possibly characterizing mm sized cortical modules, corresponds roughly to a frequency scale $40/A$ Hz, A atomic weight. The thermal stability supports the earlier idea that Z^0 force, dark neutrino superconductivity, $\nu\bar{\nu}$ wormhole contacts, and ZEG relate to cognition which must be thermally insulated whereas electromagnetic interactions would relate to sensory perception which could be highly sensitive even to temperature differences.

3. Dark neutrino super conductivity

Neutrinos play a key role in TGD based model for cognition and hearing and it is interesting to see whether this model survives the radically different interpretation of long ranged weak fields forcing to introduce large \hbar variants of $k = 113$ weak bosons. The notion of cognitive neutrino pair generalizes elegantly to $\nu\bar{\nu}$ wormhole contact such that ν is dark neutrino coupling to exotic light weak bosons. The model for quantum critical electronic superconductivity discussed in previous chapter generalizes in a rather straightforward manner and together with its electronic counterpart correctly predicts and provides interpretation for the fundamental biological length scales.

A strong deviation from the previous picture is that one must however assume that the neutrinos which are most relevant for cognition correspond to $k = 127$ and mass of order $.5$ MeV. Quantum model of hearing, which is one of the quantitative victories of TGD inspired theory of consciousness, is not affected appreciably if one requires that

the Gaussian Mersennes $k = 167, 163, 157$ label scaled down copies of charged leptons with $k = 113$ defining the mass scales of exotic weak bosons. Neutrino mass scale should be much lower than .5 eV mass of exotic electron (the metabolic energy quantum by the way) rather than .5 MeV mass scale.

The large neutrino mass scale could be understood as effective mass scale if the neutrino space-time sheets are connected by color magnetic flux tubes with $k = 127$ quarks at their ends in the same manner as nucleons form nuclear strings in TGD based model of nucleus. Also leptomesons, which have been identified as pion like bound states of color octet leptons and explain the anomalous production of electron pairs in the scattering of heavy nuclei just above Coulomb wall, could be understood as exotic $k = 167$ lepton space-time sheets connected together by color bonds having $k = 127$ quarks at their ends. There would be quark-antiquark pair per lepton making possible color octet state.

4. Atmospheric phenomena and superconductivity

There is a considerable evidence that various electromagnetic time scales associated with the atmospheric phenomena correspond to those associated with brain functioning. If magnetic sensory canvas hypothesis holds true, this is just what is expected. In this section these phenomena are considered in more detail with the aim being to build as concrete as possible vision about the dynamics involving the dark matter Bose-Einstein condensates at super-conducting magnetic and Z^0 magnetic flux quanta.

Tornadoes and hurricanes provide the first example of self-organizing systems for which Bose-Einstein condensates of dark matter at magnetic and Z^0 magnetic flux quanta might be of relevance. Auroras represent a second phenomenon possibly involving supra currents of Cooper pairs and of exotic ions. Lightnings, sprites and elves might also involve higher levels of dark matter hierarchy. p-Adic length scale hypothesis and the hierarchy of Planck constants provide a strong grasp to these far from well-understood phenomena and allow to build rather detailed models for them as well as to gain concrete understanding about how dark matter hierarchy manifests itself in the electromagnetic phenomena at the level of atmosphere.

1 Introduction

This chapter is devoted to further applications of the theory of high T_c superconductors as quantum critical superconductors involving dark matter hierarchy and large values of \hbar . The theory is applied to explain the strange

findings about ionic currents through cell membrane, exotic neutrino superconductivity and the notion of cognitive neutrino pair are discussed, and the possibility that superconductivity and Bose-Einstein condensates are involved with atmospheric phenomena is considered.

1.1 Strange behavior of cellular water and quantal ionic currents through cell membrane

The fact that cellular water does not leak out of cell in a centrifugal force suggests that some fraction of water inside cell is in different phase. One explanation is that the nuclei of water inside cell are in doubly dark phase whereas electrons are in singly dark phase (having Compton length of 5 nm and perhaps directly "visible" using day technology!) as indeed predicted by the model of high T_c superconductivity. This conceptual framework could explain various findings challenging the notions of ionic pumps.

The empirical findings challenging the notions of ionic pumps and channels, nicely summarized by G. Pollack in his book [3], provide a strong support for the notions of many-sheeted space-time and ionic superconductivity.

a) The selectivity of the cell membrane implies that channels cannot be simple sieves and there must be complex information processing involved.

b) The needed number of pumps specialized to particular ions is astronomical and the first question is where to put all these channels and pumps. On the other hand, if the cell constructs the pump or channel specialized to a given molecule only when needed, how does it know what the pump looks like if it has never seen the molecule? The needed metabolic energy to achieve all the pumping and channelling is huge. Strangely enough, pumping does not stop when cell metabolism stops.

c) One can also wonder why the ionic currents through cell membrane look quantal and are same through cell membrane and silicon rubber membrane.

These observations suggest strongly the presence non-dissipative ionic currents and quantum self-organization. The TGD based explanation would be in terms of high T_c electronic and possibly even ionic superconductivity associated with cell membrane made possible by the large \hbar phase for nuclei and electrons in the interior of cell. It however seems that thermal stability conditions allow only protonic Cooper pairs in the model of ionic Cooper pairs based on direct generalization of the model of high T_c electronic superconductivity. This does not however mean that quantal ionic currents would be absent. This empirical input also supports a view about homeostasis as a many-sheeted ionic flow equilibrium controlled by larger space-time

sheets with the mediation of massless extremals (MEs) serving as space-time correlates for Bose-Einstein condensates of massless bosons (also of scaled down dark electro-weak bosons and gluons).

In the proposed picture one can understand how extremely low densities of ions and their supra currents can control much higher ion densities at the atomic space-time sheets. The liquid crystal nature of the bio-matter is crucial for the model. This vision allows also much better understanding of the effects of ELF em fields on bio-matter. Also the effects of homeopathic remedies and acupuncture known to crucially involve electromagnetic frequency signatures of chemicals can be understood if homeostasis is based on many-sheeted ionic flow equilibrium.

1.2 Dark Z^0 magnetic fields and cognition

Similar arguments as in the em case apply in the scale $L_w=.2 \mu\text{m}$ for Z^0 magnetic transitions with scale about 10^4 eV much above the thermal energy scale. The hierarchy of length scales is now $L_w=.2 \mu\text{m}$, .4 mm, .8 m,... $L_w=.4$ mm, possibly characterizing mm sized cortical modules, corresponds roughly to a frequency scale $40/A$ Hz, A atomic weight. The thermal stability supports the earlier idea that Z^0 force, dark neutrino superconductivity, $\nu\bar{\nu}$ wormhole contacts, and ZEG relate to cognition which must be thermally insulated whereas electromagnetic interactions would relate to sensory perception which could be highly sensitive even to temperature differences.

1.2.1 How noble gases can act as anesthetes?

Chemically inert noble gases are known to act as anesthetes. Somehow these atoms affect neuronal membrane, probably reducing the nerve pulse activity. A possible explanation is in terms of anomalous weak isospin due to the charged color bonds inside nuclei of noble gas generated in the cellular environment. This bonds carry also em charge so that noble gas atom would behave like ion with nuclear charge $Z+1$ or $Z-1$. Also the long ranged color force and dark weak force with range $L_w=.2 \mu\text{m}$ associated with noble gas nuclei in dark phase could be part of the solution of the mystery.

1.2.2 Dark neutrino super conductivity

Neutrinos play a key role in TGD based model for cognition and hearing [M6] and it is interesting to see whether this model survives the radically different interpretation of long ranged weak fields forcing to introduce large \hbar variants of $k = 113$ weak bosons. The notion of cognitive neutrino pair

generalizes elegantly to $\nu\bar{\nu}$ wormhole contact such that ν is dark neutrino coupling to exotic light weak bosons. The model for quantum critical electronic superconductivity discussed in previous chapter [J1] generalizes in a rather straightforward manner and together with its electronic counterpart correctly predicts and provides interpretation for the fundamental biological length scales.

A strong deviation from the previous picture is that one must however assume that the neutrinos which are most relevant for cognition correspond to $k = 127$ and mass of order .5 MeV. Quantum model of hearing, which is one of the quantitative victories of TGD inspired theory of consciousness, is not affected appreciably if one requires that the Gaussian Mersennes $k = 167, 163, 157$ label scaled down copies of charged leptons with $k = 113$ defining the mass scales of exotic weak bosons. Neutrino mass scale should be much lower than .5 eV mass of exotic electron (the metabolic energy quantum by the way) rather than .5 MeV mass scale.

The large neutrino mass scale could be understood as effective mass scale if the neutrino space-time sheets are connected by color magnetic flux tubes with $k = 127$ quarks at their ends in the same manner as nucleons form nuclear strings in TGD based model of nucleus [F8]. Also leptomesons, which have been identified as pion like bound states of color octet leptons and explain the anomalous production of electron pairs in the scattering of heavy nuclei just above Coulomb wall [F7], could be understood as exotic $k = 167$ lepton space-time sheets connected together by color bonds having $k = 127$ quarks at their ends. There would be quark-antiquark pair per lepton making possible color octet state.

1.3 Atmospheric phenomena and superconductivity

There is a considerable evidence that various electromagnetic time scales associated with the atmospheric phenomena correspond to those associated with brain functioning. If magnetic sensory canvas hypothesis holds true, this is just what is expected. In this section these phenomena are considered in more detail with the aim being to build as concrete as possible vision about the dynamics involving the dark matter Bose-Einstein condensates at super-conducting magnetic and Z^0 magnetic flux quanta.

Tornadoes and hurricanes provide the first example of self-organizing systems for which Bose-Einstein condensates of dark matter at magnetic and Z^0 magnetic flux quanta might be of relevance. Auroras represent a second phenomenon possibly involving supra currents of Cooper pairs and of exotic ions. Lightnings, sprites and elves might also involve higher levels

of dark matter hierarchy. p-Adic length scale hypothesis and the hierarchy of Planck constants provide a strong grasp to these far from well-understood phenomena and allow to build rather detailed models for them as well as to gain concrete understanding about how dark matter hierarchy manifests itself in the electromagnetic phenomena at the level of atmosphere.

2 Empirical support for ionic super-conductivity as a fundamental control mechanism

The notions of ionic channels and pumps associated with cell membrane are central for the standard cell biology [8]. There are however puzzling observations challenging this dogma and suggesting that the currents between cell interior and exterior have quantum nature and are universal in the sense that they not depend on the cell membrane at all [4, 5, 22, 9, 10]. One of the pioneers in the field has been Gilbert Ling [4], who has devoted for more than three decades to the problem, developed ingenious experiments, and written several books about the topic. The introduction of the book [3]) gives an excellent layman summary about the paradoxical experimental results¹.

It was a pleasant surprise to find that these experimental findings give direct support for the role of supra currents and Josephson currents in bio-control. In fact, the experimental data lead to an archetype model cell homeostasis as a flow equilibrium in which very small densities of super-conducting ions (also molecular ions) and ionic supra currents at cellular and other super-conducting space-time sheets dictate the corresponding densities at the atomic space-time sheets. Z^0 super-conductivity in principle allows to generalize the model also to the control of the densities of neural atoms and molecules at atomic space-time sheets.

2.1 Strange behavior of the intracellular water

The basic strange feature of cellular interior is related to its gelatinous nature and is in fact familiar for everyone. Although 80 percent of hamburger is water, it is extremely difficult to extract this water out. Ling [5] has demonstrated this at cellular level by using a centrifuge and cells for which cell membrane is cut open: centrifugal accelerations as high as 1000 g fail to induce the separation of the intracellular water.

¹I am grateful for 'Wandsqueen' for sending me the relevant URL address and for Gene Johnson for very stimulating discussions.

The dipolar nature of biomolecules and induced polarization are basis prerequisites for the formation of gels. Ling raises the cohesion between water and protein molecules caused by electric dipole forces as a fundamental principle and calls this principle association-induction hypothesis [4]. This cohesion gives rise to liquid crystal [13] like structure of water implying among other things layered structures and internal electric fields orthogonal to the plane of the layers [4, 11, 12]. For instance, cell membranes can be understood as resulting from the self-organization of liquid crystals [13]. The fundamental importance of electret nature of biomatter was also realized by Fröhlich [14] and led him to suggest that macroscopic quantum phases of electric dipoles might be possible. This concept, which is in central role in many theories of quantum consciousness, has not been established empirically.

2.2 Are channels and pumps really there?

Standard neurophysiology relies strongly on the concepts of what might be called hydro-electro-chemistry. The development of the theory has occurred through gradual improvements saving the existing theory.

The development began from the basic observation that cells are stable gelatinous entities not mixing with the surrounding water. This led to the hypothesis that cell membrane takes care that the contents of the cell do not mix with the cell exterior. It was however soon found that cell membrane allows some ions to flow through. The interaction between theory and experiment led gradually to the notions of ion channel and ion pump, which are still central for the standard paradigm of the cell [8]. Note that also 'electric pump' taking care that membrane potential is preserved, is needed.

These notions developed gradually during the period when cell was seen as a bag containing water and a mixture of various biochemicals. If cell biology would have started to develop during the latter half of this century and after the discovery of DNA, cell as a computer metaphor might have led to a quite different conceptualization for what happens in the vicinity of the cell membrane. Also the notion of liquid crystals [13] would have probably led to different ideas about how homeostasis between cell interior and exterior is realized [4, 11, 12].

For me it was quite a surprise to find that pump-channel paradigm is not at all so well-established as I had believed as an innocent and ignorant outsider. The first chapter of the book "Cells, Gels and the Engines of Life" of Gerald Pollack [3] provides a summary about the experimental paradoxes (the interested reader can find the first chapter of this book from web).

The standard theoretical picture about cell is based on the observation that cell exterior and interior are in a relative non-equilibrium. The measured concentrations of various atomic ions and organic molecules are in general different in the interior and exterior and cell membrane seems to behave like a semi-permeable membrane. There is also a very strong electric field over the cell membrane. In standard approach, which emerged around 1940, one can understand the situation by assuming that there are cell membrane pumps pumping ions from cell interior to exterior or vice versa and channels through which the ions can leak back. Quite a many candidates for proteins which seem to function like pump and channel proteins have been identified: even a pump protein for water [3]! This does not however prove that pumping and channelling is the main function of these proteins or that they have anything to do with how ionic and molecular concentrations in the interior and exterior of the cell are determined. It could quite well be that pump and channel proteins are receptors involved with the transfer of information rather than charges and only effectively act as pumps and channels.

There are several serious objections of principle against the vision of cell as a bag of water containing a mixture of chemicals. Even worse, the hypothesis seems to be in conflict with experimental data.

2.2.1 Selectivity problem

Cell membrane is extremely selective and this leads to an inflation in the complexity of channels and pumps. The problem might be christened as a dog-door problem: the door for dog allows also cat go through it. Channels cannot be simple sieves: it is known that channels which let some ions through do not let much smaller ions through. There must be more complicated criteria than geometric size for whether the channel lets the ion go through. Quite generally, channels must be highly selective and this seems to require complicated information processing to decide which ion goes through and which not. As a consequence, the models for channels inflate in their complexity.

The only reasonable way to circumvent the problem is to assume that there is kind of binary coding of various chemical compounds but it is difficult to see how this could be achieved in the framework of the standard chemistry. The notion of N-atom proposed in [J6] to give rise to the emergence of symbols at the level of biochemistry could however allow this kind of coding. Channels and pumps (or whatever these structures actually are) could be also generated by self-organization process when needed.

2.2.2 Inflation in the number of pumps and channels

Channels and pumps for atomic ions and channels and pumps for an astronomical number of organic molecules are needed. The first question is where to put all those channels and pumps? Of course, one could think that pumps and channels are constructed by the cell only when they are needed. But how does the cell know when a new pump is needed if the cell as never met the molecule in question: for instance, antibiotic or curare molecule?

To realize how weird the picture based on channels and pumps is, it is useful to imagine a hotel in which there is a door for every possible client letting only that client through but no one else. This strange hotel would have separate door for every five point five milliard humans. Alternatively, the building would be in a continual state of renovation, new doors being built and old being blocked.

There is however an TGD based objection against this slightly arrogant argument. In TGD framework cell is a self-organizing structure and it might be that there is some mechanism which forces the cell to produce these pumps and channels by self-organization. Perhaps the basic characteristic of quantum control in many-sheeted space-time is that it somehow forces this kind of miracles to occur.

2.2.3 Why pumping does not stop when metabolism stops?

One can also wonder how metabolism is able to provide the needed energy to this continual construction of pumps and channels and also do the pumping. For instance, sodium pump alone is estimated to take 45-50 per cent of the cell's metabolic energy supply. Ling has studied the viability of the notion of the ionic pump experimentally [4] by exposing cell to a cocktail of metabolic poisons and depriving it from oxygen: this should stop the metabolic activities of the cell and stop also the pumping. Rather remarkably, nothing happened to the concentration gradients! Presumably this is the case also for the membrane potential so that also the notion of metabolically driven electrostatic pumps seems to fail. Of course, some metabolism is needed to keep the equilibrium but the mechanism does not seem to be a molecular mechanism and somehow manages to use extremely small amount of metabolic energy.

2.2.4 How it is possible that ionic currents through silicon rubber membrane are similar to those through cell membrane?

A crucial verification of the channel concept was thought to come in the experiment of Neher and Sakmann [7] (which led to a Nobel prize). The ingenious experimental arrangement was following. A patch of membrane is sucked from the cell and remains stuck on the micropipet orifice. A steady voltage is applied over the patch of the membrane and the resulting current is measured. It was found that the current consists of discrete pulses in consistency with the assumption that that a genuine quantum level current is in question. The observation was taken as a direct evidence for the postulate that the ionic currents through the cell membrane flow through ionic channels.

The later experiments of Fred Sachs [9] however yielded a complete surprise. Sachs found that when the patch of the cell membrane was replaced by a patch of silicon rubber, the discrete currents did not disappear: they remained essentially indistinguishable from cell membrane currents! Even more surprisingly, the silicon rubber membrane showed ion-selectivity features, which were essentially same as those of the cell membrane! Also the currents through synthetic polymer filters [10] were found to have essentially similar properties: as if ion selectivity, reversal potential, and ionic gating would not depend at all on the structure of the membrane and were more or less universal properties. Also experiments with pure lipid-layer membranes [22] containing no channel proteins demonstrated that the basic features – including step conductance changes, flickering, ion selectivity, and in-activation– characterized also cell membranes containing no ionic channels.

The in-escapable conclusion forced by these results seems to be that the existing 60-year old paradigm is somehow wrong. Ionic currents and the their properties seem to be universal and depend only on very weakly on the properties of the membrane.

2.3 Could the notion of the many-sheeted space-time solve the paradoxes?

The basic paradoxes are related to the universality of the ionic currents suggesting the absence of ionic channels and to the absence of metabolically driven chemical pumps assignable to cell membrane. Chemical pumps take care that the differences of the chemical potentials associated with the two sides of the cell membrane remain non-vanishing just like ordinary pump pre-

serves a constant pressure difference. Also 'electrical pump' taking care that the potential difference between the cell exterior and interior is preserved is needed. The experiments suggest strongly that both chemical pumps and 'electrical pump', if present at all, need very low metabolic energy feed.

Many-sheeted space-time allows following interpretation for the puzzling findings.

a) What have been identified as pumps and channels are actually ionic receptors allowing the cell to measure various ionic currents flowing through membrane.

b) Pumps are not needed because the cell interior and exterior correspond to disjoint space-time sheets. The currents run only when join along boundaries contact (JAB) is formed and makes the current flow possible. The fact that the formation of JABs is quantal process explains the quantal nature of the currents. Channels are not needed because the currents run as supra currents (also the cyclotron states of bosonic ions define Bose-Einstein condensates) along cell membrane space-time sheet. The absence of dissipation would explain why so little metabolic energy feed is needed and why the ionic currents are not changed when the cell membrane is replaced by some other membrane. JABs could be formed between the space-time sheets representing lipid layers or between cell exterior/interior and cell membrane space-time sheet. The formation of JABs has also interpretation as a space-time correlate for the generation of quantum entanglement.

c) The universality of the currents suggests that the densities of current carriers are universal. The first interpretation would be in terms of an ordinary-dark-ordinary phase transition. Ordinary charge carriers at space-time sheets associated with cell interior and exterior would be transformed to dark matter particles at the cell membrane space-time sheet and flow through it as supra currents and then transform back to ordinary particles (reader is encouraged to visualize the different space-time sheets). This phase transition could give for the currents their quantal character instead of the formation of JABs. Of course, the formation of JABs might be prerequisite for this phase transition.

d) The ion densities in cell interior and exterior are determined by flow equilibrium conditions for currents traversing from super-conducting space-time sheets to non-super-conducting space-time sheets and back. Ion densities would be controlled by super-conducting ion densities by an amplification mechanism made possible by the electret nature of the liquid crystal state. The dissipation by the currents at the atomic space-time sheets associated with cell interior and exterior is very weak by the weakness of the electric fields involved and at cell membrane space-time sheet superconduc-

tivity means absence of dissipation.

2.3.1 Many-sheeted cell

TGD based model of nerve pulse and EEG relies on the notion of the many-sheeted space-time. There is entire hierarchy of space-time sheets so that one can assign to cell and its exterior atomic space-time sheets forming join-along boundaries condensate of units of size of about 10^{-10} meters, lipid layer *resp.* cell membrane space-time sheets with thickness of order $L(149) \simeq .5 \times 10^{-8}$ meters *resp.* $L(151) \simeq 10^{-8}$ meters, and cellular space-time sheets with size of order few microns. These space-time sheets are certainly not the only ones but the most important ones in the model of EEG and nerve pulse.

a) Water molecules at the atomic space-time sheet can form join along boundaries bond condensates and the strange properties of water inside the cell can be understood if these lumps in the cell interior have size larger than the join along boundaries bonds connecting atomic space-time sheet of cell interior to that of cell exterior. Liquid crystal structure indeed gives rise to layered crystal like structures of water.

b) Cell membrane space-time sheets have size of order cell membrane thickness and are assumed to be super-conducting. The lipid layers of the cell membrane define space-time sheets of thickness of about 50 Angstrom, which could act as parallel super-conductors connected by Josephson junctions.

c) Cellular space-time sheets have size of order cell size and are multi-ion super-conductors. Also they are connected to each other by join along boundaries bonds serving as Josephson junctions. Also charged organic molecules could form super-conductors and be transferred by the same mechanism between cell interior and exterior. In TGD framework also classical Z^0 fields are present and Z^0 super-conductivity is possible and could make possible neutral supra currents and control of the densities of the neutral atoms and molecules.

Neuronal and cellular space-time sheets of size of order cell size are assumed to be parts of the magnetic flux tube like structures associated with Earth's magnetic field. Earth's magnetic field inside organisms could contain closed circuits and it is conceivable that the notion of magnetic circulation containing neural circuitry as a sub-circuitry makes sense. Large value of \hbar makes possible high T_c superconductivity. Only protonic Cooper pairs are possible at room temperature besides electronic and neutrino Cooper pairs using the proposed criterion super conductivity. Bose-Einstein condensates of bosonic ions at cyclotron states define also superconductors and at $k = 4$

level of dark matter hierarchy the cyclotron frequencies in Earth's magnetic field correspond to energies above thermal energy. These frequencies are in alpha band for most biologically relevant bosonic ions.

Electronic Josephson currents through cell membrane oscillate with a frequency which is given by the membrane potential $eV = 70 \text{ meV}$: this predicts that the emission of infrared photons as a signature of a living cell. Super currents transform to Ohmic currents when they enter to the atomic space-time sheets.

Also present are 'many-sheeted circuits' for which currents flow along super-conducting space-time sheets go to atomic space-time sheets where they flow as very weak Ohmic currents, and run back to super-conducting space-time sheets. The currents flowing in closed circuits traversing both cellular and atomic space-time sheets are in flow equilibrium. Because of the high value of the cell membrane electric field, the ionic currents flowing at cell membrane space-time sheets would give rise to high dissipation. The ohmic currents from the cell exterior to interior can however enter to the super-conducting cell membrane space-time sheet and back to the atomic space-time sheet of the cell interior and thus avoid the dissipation.

This picture suggests that the flow of particles between the cell interior and exterior takes mainly via the cell membrane space-time sheet. This would mean that $k = 169$ cell interior space-time sheet has permanent bridges to the $k = 151$ cell membrane space-time sheet, which in turn has only temporary bridges to the $k = 169$ cell exterior space-time sheets.

The character of the ionic currents through cell membrane is highly relevant for the model of the nerve pulse. The development of the model of nerve pulse [M2] has taken a long time and the original hypothesis about the decisive role of the ionic Josephson currents turned out to be wrong. The recent version of the model assumes that the reduction of charge entanglement between magnetic body and neuron interior made possible by charged W MEs leads to a exotic ionization of the Ca^{++} Bose-Einstein condensate. Exotic $Ca^{++,+}$ Bose-Einstein condensate reduces the membrane resting potential below the threshold for the generation of nerve pulse. The random generation of JABs makes possible flow of ionic currents and leads to the generation of nerve pulse. One cannot exclude the possibility that a portion of em or Z^0 ME drifting along the axon with the velocity of nerve pulse and connecting cell exterior and cell membrane space-time sheets defines the JAB: in the earlier version of the model Z^0 ME was responsible for the reduction of the membrane potential.

2.3.2 Faraday's law of induction in the many-sheeted space-time forces electrical non-equilibrium

Faraday's induction law in many-sheeted space-time gives strong constraints on the electric fields over the cell membrane region at various space-time sheets. Suppose that cellular space-time sheet and some other space-time sheets, say cellular and cell membrane space-time sheet, are in contact so that one can form a closed loops traversing along both space-time sheets. Faraday's law implies that the rotation of electric field around a closed loop traversing first from cell exterior to interior at cellular space-time sheet, going to the atomic space-time sheet and returning back to cell exterior and down to cellular space-time sheet must be equal to the time derivative of the magnetic flux through this loop. Since magnetic flux cannot grow indefinitely, the time average of this potential difference is vanishing. During the generation of nerve pulse the situation might change but only for a finite duration of time (of order millisecond).

Thus in electrostatic equilibrium there must be same exterior-interior potential difference over all space-time sheets in contact with cellular space-time sheets and the variation of potential difference at cellular space-time sheets induces automatically an opposite variation at other space-time sheets. This means that the supra currents at cellular space-time sheets can indeed control potential differences at other space-time sheets, in particular at atomic space-time sheets. Faraday's law in the many-sheeted space-time also implies that Ohmic currents at atomic space-time sheets cannot destroy the potential difference except for a finite period of time.

Faraday's law makes also possible a gauge interaction between dark and ordinary matter. The changes of dark matter charge densities induce changes of electric field patterns at dark matter space-time and once JABs are formed between dark matter space-time sheet and space-time sheets at lower level of dark matter hierarchy, closed many-sheeted circuits become possible and voltage differences along space-time sheet at different levels of dark matter hierarchy correspond to each other.

Massless extremals (MEs, topological light rays) serve as correlates for dark bosons. Besides neutral massless extremals (em and Z^0 MEs) TGD predicts also charged massless extremals obtained from their neutral counterparts by a mere color rotation (color and weak quantum numbers are not totally independent in TGD framework). The interpretation of the charged MEs has remained open hitherto. Charged W MEs could induce long length scale charge entanglement of Bose-Einstein condensates by inducing exotic ionization of ionic nuclei. State function reduction could lead to a state

containing a Bose-Einstein condensate in exotically ionized state.

In this manner the charge inside neuron and thus by Faraday's law membrane potential could be affected by magnetic body. The generation of nerve pulse could rely on the reduction of the resting potential below the critical value by this kind of mechanism inducing charge transfer between cell interior and exterior. The mechanism might apply even in the scale of magnetic body and make possible the control of central nervous system. Also remote mental interactions, in particular telekinesis, might rely on this mechanism.

2.3.3 Flow equilibrium in many-sheeted space-time

The notion of many-sheeted space-time suggests that cell interior and exterior could be regarded as a system in 'many-sheeted flow equilibrium' so that the ion densities at atomic space-time sheets are determined by the ion densities at the super-conducting cellular space-time sheets and by the drift velocities by the basic formula $n_1/n_2 = v_2/v_1$ for flow equilibrium.

a) Cell exterior and interior understood as many-sheeted structures are in ionic flow equilibrium holding true for each ion type. The ionic currents run along circuits which traverse along super-conducting space-time sheets, enter into atomic space-time sheets and back to super-conducting space-time sheets.

b) To understand what is involved consider the simplest possible closed circuit connecting atomic and cellular space-time sheets. The ionic super-current $I_{i,s}$ flowing from a super-conducting space-time sheet to the atomic space-time sheet is transformed to Ohmic current $I_{i,O}$ in the atomic space-time sheet and in flow equilibrium one has

$$I_{i,s}(int) = I_{i,s} = I_{i,O}(ext) = I_i(membr) .$$

c) Ionic supra current is sum of two terms.

$$I_{i,s} = I_{i,s|J} + I_{i,s|d} .$$

The first term is the oscillatory Josephson current associated with the Josephson junction connecting interior and exterior cellular space-time sheet. The second term is direct supra current

$$I_{i,s|d} = \frac{1}{m_i} n_{i,s} \nabla \phi = \frac{n_{i,s} K_i}{m_i} ,$$

where ϕ is the phase of the super-conducting order parameter, and m_i is the mass of the ion. K_i is the quantized momentum like quantum number

associated of super conducting loop (assuming for simplicity that current is constant).

d) Ionic Ohmic current is equal to

$$I_{i,O}(int) = \frac{n_i(int)q_i E_{int}}{k_i(int)} ,$$

$$I_{i,O}(ext) = \frac{n_i(ext)q_i E_{ext}}{k_i(ext)} .$$

Here k_i is linear friction coefficient. Since cell exterior and interior are in different internal states, k_i is different for cell interior and exterior. E is the weak internal electric field made possible by liquid crystal property which is also different for the interior and exterior. Flow equilibrium conditions give for the ratio of the ion densities in interior and exterior

$$\frac{n_i(int)}{n_i(ext)} = \frac{v_i(ext)}{v_i(int)} = \frac{E_{ext} k_i(int)}{E_{int} k_i(ext)} .$$

Thus in flow equilibrium the ratio of the internal and external ion densities differs from unity and is determined by the ratio of the ionic drift velocities, which are different in cell interior and exterior.

e) The densities of the super-conducting ions at super-conducting space-time sheet determine the corresponding ion densities at the atomic space-time sheet

$$\frac{n_i(int)}{n_{i,s}} = \frac{v_{i,s}}{v_i(int)} = \frac{K_i k_i(int)}{m_i E_{int}} ,$$

$$\frac{n_i(ext)}{n_{i,s}} = \frac{v_{i,s}}{v_i(ext)} = \frac{K_i k_i(ext)}{m_i E_{ext}} .$$

Obviously, super-conducting ion densities control the ion densities at the atomic space-time sheets. Very weak electric fields E_{ext} and E_{int} and high values of friction coefficients k_i make possible a large amplification of the super conducting densities to the non-super-conducting ionic densities at atomic space-time sheet. Thus the fact that liquid crystals allow weak but stable electric fields orthogonal to the layer like structure is crucial for the mechanism.

f) Also flow equilibrium requires metabolism to keep the currents at the atomic space-time sheets flowing. There are two options.

i) Assuming that the current flows through cell membrane as an Ohmic current, the power dissipated in the circuit is equal to

$$P = I_i(int)(V_{int} + V_{memb} + V_{ext}) = I_{i,s}(V_{int} + V_{memb} + V_{ext}) .$$

Since supercurrents and thus also Ohmic currents are weak and electric fields are weak in cell interior and exterior, also dissipation can be extremely low in these regions. The dominating and problematic term to the dissipation comes from the membrane potential which is very large.

ii) An alternative option is that the current flows through cell membrane region as a supercurrent by going from atomic to cell membrane space-time sheet and returning back to atomic space-time sheet. This gives

$$P = I_{i,s}(V_{int} + V_{ext}) .$$

In this manner huge amount of metabolic energy would be saved and it is quite possible that this is the only sensible manner to understand the experimental results of Ling [4].

2.3.4 Refinements and generalizations

The proposed oversimplified model allows obviously refinements and variants. For instance, current circuits could run from exterior cellular space-time sheet to cell membrane space-time sheet and run only through the cell interior. In this case only the ionic concentrations in the cell interior would be controlled: this does not look a good idea. This option might be necessary in the case that cell exterior cannot be regarded as an electret carrying weak but stable electric field.

Several super-conducting space-time sheets are probably involved with the control and complex super-conducting circuits are certainly involved. The structure of the cell interior suggests a highly organized ohmic circuitry. In particular, cytoskeleton could be important carrier of currents and atomic space-times sheets of the microtubules could be in crucial role as carriers of the ohmic currents: there is indeed electric field along microtubule. The collagenous liquid crystalline networks [11, 12] are excellent candidates for the carriers of weak ohmic currents in the inter-cellular tissue. Fractality suggests that also structures like proteins, DNA and microtubules are in a similar flow equilibrium controlled by super-conducting ion densities at protein/DNA/microtubule space-time sheets and probably also larger space-time sheets.

Bioelectromagnetic research provides a lot of empirical evidence for the existence of the direct current ohmic circuits, mention only the pioneering work of Becker and the work of Nordenström [2, 20]. For instance, these direct currents are proposed to be crucial for the understanding of the effects of the acupuncture. The ancient acupuncture, which even now is not taken seriously by many skeptics, could indeed affect directly the densities

and supercurrents of ions at super-conducting space-time sheets and, rather ironically, be an example of genuine quantum medicine.

2.3.5 Explanation of the paradoxes in terms of many-sheeted space-time

The qualitative predictions of the flow equilibrium model conform with the experimental facts discussed above.

a) One can understand how a gelatinous lump of matter can be a stable structure if the interior of the cell is in a gelatinous state in length scales larger than the size of the Josephson junctions at atomic space-time sheet. This means that water inside cell consists of coherent lumps larger than the size of Josephson junction and cannot leak to the exterior. If the exterior of the cell forms single large space-time sheet or consists of sheets connected by Josephson junctions with size larger than the typical size for the coherent lumps of water in cell exterior, cell exterior behaves like ordinary mixture of water and chemicals.

b) The amplification mechanism of supra currents relying crucially on liquid crystal property implies that although liquid crystal pumps and metabolism are needed, the amount of metabolic energy can be extremely small. Absolutely essential is however that ohmic currents run through the super-conducting short circuit provided by the cell membrane space-time sheet.

c) The currents for various ions do not depend at all on the properties of the cell membrane but are determined by what happens on cellular and other super conducting space-time sheets. In flow equilibrium supra currents and Josephson currents are identical with currents through cell membrane at atomic space-time sheet. The observed quantal nature of the ionic currents supports their interpretation as faithful atomic level images of supra currents.

d) Since various ionic currents at the cellular space-time sheets dictate the ionic currents at the atomic space-time sheets, the selectivity of the cell membrane would seem to be only an apparent phenomenon. One must however be very cautious here. The self-organizing cell membrane might have the virtue of being co-operative and develop gradually structures which make it easier to establish the flow equilibrium. For large deviations from the flow equilibrium, ohmic currents are expected to flow through the atomic space-time sheet associated with the cell membrane since super-conducting currents become overcritical and super-conductivity is spoiled. Also the proteinic Josephson junctions between lipid layer space-time sheets might be crucial. Thus the notions of channel and pump proteins might make

sense in the far from flow equilibrium regime where the currents though membrane region are dominantly ohmic.

To sum up, one could see super-conducting space-time sheets as controllers of the evolution of the cellular and other biological structures and the model of organism could be specified to some degree in terms of the densities and currents of the super-conducting particles at various space-time sheets besides the values quantized magnetic fluxes associated with various many-sheeted loops. Setting up the goal at controlling space-time sheets would force the atomic space-time sheets to self-organize so that the goal is achieved. This clearly provides a quantum mechanism of of volition. A fascinating challenge is to apply this vision systematically to understand morphogenesis and homeostasis.

Needless to say, the notion of many-sheeted current circuitry would have also revolutionary technological implications since all undesired dissipative effects could be minimized and currents at atomic space-time sheets would be used only for heating purposes! Of course, many-sheeted current circuitries would also make possible quantum computer technologies.

2.3.6 Bio-control as a control of quantum numbers characterizing supracurrents

The magnetic quantum numbers K_i which together with the densities of super-conducting ions characterize the densities of various ions at atomic space-time sheets. Thus magnetic quantum numbers associated with super-conducting circuits formed by magnetic flux tubes indeed characterize biological information as speculated already more than decade ago on basis of mathematical necessity. Direct ohmic currents and supra currents determine these quantum numbers only partially since in super-conducting circuit integer valued magnetic flux can flow without any induced current in the circuit. In presence of dissipation the currents in super-conducting circuit are minimal needed to guarantee quantized flux through the circuit.

In this picture biocontrol boils down to the changing of the various integers characterizing the phase increments over closed super conducting loops. If nerve pulse involves induction of supra curent compensating the deviation of the magnetic flux in circuit from integer multiple of flux quantum, this can be achieved. The coupling of super-conducting circuits with MEs makes it possible for MEs to affect the magnetic quantum numbers by time varying or constant magnetic fields.

a) If dissipation is slow, supra currents and thus also ionic concentrations can suffer a large change and the homeostatis of neuron changes for a period

determined by the rate of dissipation for supra currents.

b) The induced supra current could also dissipate rapidly to minimal supra current required by the quantization of the magnetic flux: the quantized part of the magnetic flux of external perturbation penetrates to super-conductor and is expected to affect the super-conducting part of the system. This does not of course occur permanently for oscillating em fields. The deviation of the external magnetic flux from a quantized value is coded to a small supercurrent. This mechanism combined with stochastic resonance possible for SQUID type circuits [24] makes it possible to 'measure' extremely weak magnetic fields of MEs by amplifying them to biological effects.

MEs can also form junctions (possibly Josephson-) between two super-conducting circuits. In this case a constant electric field associated by ME defines the frequency of the induced Josephson current: the weaker the potential difference, the slower the oscillation period. This mechanism might explain why the effects of ELF em fields in living matter occur in intensity windows.

2.3.7 The role of the cell membrane

What is the role of the cell membrane in TGD inspired picture about cell? Very much what it is found to be. Cell membrane recognizes various organic molecules, interacts with them, and possibly allows them to go through. A protein in the cell membrane might act as an effective channel or pump but this function would be only apparent in case of ions. Only if cell membrane space-time sheet has join along boundaries contacts with the cell interior, can ions and proteins enter cell interior through the membrane space-time sheet. One must also consider very seriously the possibility that cell membrane space-time sheet is a carrier of supra currents participating in the control of the physics at atomic space-time sheets.

This vision conforms with a computer-ageist view about cell membrane as an interface between computer and clients. Against the fact that tools (proteins) and symbols (DNA) emerge already at atomic length scale, it would indeed seem rather strange that cell would reduce to a bag of water containing mixture of chemicals. This view conforms also with fractality. Skin is the largest connected part of the nervous system and cell membrane could be also seen as the skin of neuron and thus a part of the nervous system of cell, specialized to receive signals from the external world.

In this vision cell is much more like a living, intelligent computer than a sack of ion-rich water, and cell membrane is its interface with the external world. Proteins and biomolecules are messages/messengers, and cell mem-

brane allows them to attach to the receptor only if a number of conditions are satisfied.

In many cases it is not necessary for the messenger to continue its travel to the interior since electromagnetic and electromechanical communications with the cell nucleus are possible by liquid crystal property of cell structures. TGD suggests MEs ('massless extremals') and magnetic flux tubes carrying ionic super-conductors as a universal tool for these communications, and the simplest hypothesis is that the fractally scaled down versions of the communications in the cell length scale are realized also in the interior of the cell and inside cell nucleus, and even at the level of DNA. The interaction of MES and topologically quantized magnetic fields could solve many of the paradoxical features related with the phenomenon of pleiotropy discussed briefly in [J4]. In particular, electromagnetic passwords and commands analogous to computer language commands based on suitable frequency combinations or even amplitude modulated field patterns could be involved. For instance, in case of DNA SQUID type mechanism combined with stochastic resonance could make possible the activation of specified genes by using specific frequency combinations associated with MEs.

2.4 Water memory, homeopathy, and acupuncture

Further guidelines for TGD based view about biocontrol and coordination were provided by the empirical evidence for water memory and various effects involved with it [18, 19, 16, 17]. In [K5] a detailed mechanism of homeopathy and water memory based on the model of biocontrol in terms of many-sheeted ionic flow equilibrium is discussed.

1. Transfer of homeopathic potency to non-atomic space-time sheets is not enough

Many-sheeted ionic flow equilibrium suggests a possible mechanism of homeopathy: the extremely low densities of homeopathic remedies are at the controlling super-conducting space-time sheets where the control is. Thus homeopathy could be seen as a high precision medicine minimizing the amount of the remedy needed rather than some kind of magic treatment. This cannot be however the whole story. As already explained the study of homeopathic effects suggest an electromagnetic representation of the biomolecules based on frequencies [17] and it is possible achieve the healing effect by transferring mere frequencies instead of using homeopathic potency.

2. Mechanisms of frequency imprinting and entrainment

According to [17], the homeopathic remedies seem to be characterized

by frequencies varying in the range containing at least the range $10^{-3} - 10^9$ Hz suggesting that electromagnetic fields at specific frequencies characterize the homeopathic remedy. These frequencies can be imprinted into water and also erased. Rather remarkably, the removal of Earth's magnetic field erases the imprinted frequencies.

On the other hand, the studies of acupuncture support the existence of certain highly coherent endogenous frequencies [17] at which electromagnetic radiation has strong effects. The fact that these frequencies can entrain to exogenous frequencies suggests a mechanism of homeopathy based on entrainment. Effects are observed at pairs of high and low frequencies and the ratio of these frequencies is constant over all acupuncture meridians with a standard deviation of ± 15 per cent. The first branch is at GHz range: in particular the frequencies 2.664 GHz, 1.42 GHz and 384 MHz have unexpected properties. The second branch of frequencies is in ELF range, in particular Schumann frequency 7.8 Hz accompanies 384 MHz.

Consider now the explanation of the observations of Smith and others in the TGD framework using the proposed model assigning to magnetic flux tubes parallel MEs making magnetic flux tube effectively a magnetic mirror.

a) The basic idea is that water forms representations for chemicals it contains in terms of transition frequencies of the chemical which become frequencies of MEs and structures of water generating these MEs by emission and absorption processes. Also representations of representations are possible. The molecule of a homeopathic potency is characterized by characteristic frequencies associated with its transitions as well as ELF frequencies. Of course, also transitions of a complex formed by molecule of the potency and water molecule could be involved.

Water represents the transition frequencies of the potency molecule as transition frequencies of water molecules or of structures which correspond to space-time sheets of various sizes. This conforms with the fact that frequency imprinting disappears after thorough drying and returns when water is added and that also bulk water without any potency allows frequency imprinting. In the frequency range studied by Smith rotational transition frequencies of water and of the space-time sheets containing water in liquid crystal form provide a good candidate for a representational mechanism. ELF frequencies correspond now to the magnetic transitions of these space-time sheets behaving like point like objects in Earth's magnetic field.

b) The simplest assumption is that the ELF branch of the frequency spectrum corresponds to the magnetic transition frequencies in Earth's magnetic field whereas the high frequency branch corresponds to the characteristic frequencies $f = c/L$ of MEs parallel to the magnetic flux tubes. This

assumption conforms with the crucial role of Earth's magnetic field in the erasure of the imprinted frequencies. Also the importance of 7.8 Hz Schumann frequency for the heart chakra [17] can be understood.

The singly ionized Ca, Ar, and K (all 7.5 Hz for $B = .5 \times 10^{-4}$ Tesla) and Cl (8.5 Hz) have cyclotron transition frequencies near to Schumann frequency. For LC water blobs the ELF frequencies are below 1 Hz and the requirement that water blob has size smaller than radius of magnetic flux tube of Earth's magnetic field allows ELF frequencies down to $1/f \sim 1000$ years so that all biologically relevant length scales are covered. Quite interestingly, the frequency f_h corresponding 1000 years is 20 Hz by the scaling law suggested by Smith and corresponds to the lower bound for audible frequencies and that also language involves subneuronal mimicry by LC water blobs. A fascinating possibility is that subneuronal LC water blobs could be responsible for all biorhythms and be involved also with our long term memories.

c) Frequency entrainment for both ELF and high frequency branches can be understood if both the thickness and length of the magnetic flux tubes are subject to a homeostatic control. The assumption that the total magnetic energy of the flux tube remains constant during the frequency entrainment together with the magnetic flux quantization implies that the ratio S/L of the area S of the magnetic flux tube to its length L remains constant during entrainment. Thus the ratios f_h/f_{ELF} of the magnetic transition frequencies to characteristic frequencies of MEs would be homeostatic invariants in agreement with the empirical findings. The value of the ratio is in good approximation $f_h/f_{ELF} = 2 \times 10^{11}$.

d) The electromagnetic signature of the homeopathic potency corresponds to MEs stimulated by the electromagnetic transitions associated with the potency molecule. Since these frequencies are also transition frequencies for water molecules or space-time sheets containing water in liquid crystal form a resonant interaction is possible and em fields of MEs can be amplified/replicated by the transitions associated with these structures.

e) According to [17], coherence propagates with a light velocity whereas coherent domain of size L diffuses with a velocity given by the scaling law $v \propto Lf$. In TGD the natural interpretation for the velocity of coherence propagation is as a signal velocity inside ME (possibly representing external em field). v is in turn associated with the motion of ME transversal to some linear structure along it: this effect is not possible in Maxwell's theory since particle-field duality is not realized at the classical level. The velocities are reported to be of order few meters per second and of the same order of magnitude as nerve pulse conduction velocity and phase velocities for EEG

waves. This relationship is of the same form as the scaling law which relates together the phase velocity of EEG wave (velocity of EEG ME in TGD framework) and the size L of corresponding structure of brain or body. For instance, scaling law relates the size L for brain structures and corresponding magnetic sensory canvas with much larger size $L_c = c/f$ [M4]. Scaling law would give $v/c = f_{ELF}/f_h$ and velocity of order mm/s for the motion of transversal MEs along magnetic flux tubes: this velocity is considerably smaller velocity than m/s reported in [17].

A detailed model for various homeopathic effects is discussed in [K5]. The model leads to a generalization of the view about many-sheeted DNA with magnetic mirrors transversal to DNA coding the electromagnetic structure of the organism and allows to understand introns as chemically passive but electromagnetically active genes. Magnetic mirrors provide also a recognition mechanism fundamental for the functioning of the bio-system: consider only the ability of aminoacids to find corresponding RNA triplets, the self assembly of tobacco mosaic virus and the functioning of the immune system. Magnetic mirrors can also serve as bridges between sender and receiver of intent in remote healing and viewing and these processes could be seen as scaled-up version of those occurring routinely endogenously.

3 Dark neutrino super conductivity

The new view about dark neutrino super conductivity differs completely in details from the earlier one. The reason is the new interpretation for classical long ranged weak gauge fields as space-time correlates for a hierarchy of exotic weak bosons with scaled down mass scale. The model of dark neutrino superconductivity will be constructed using various empirical guidelines about neutrinos to set quantitative constraints. The model itself is a direct generalization of the model for quantum critical electronic super conductor based on wormhole Cooper pairs generalized to the case of ORMEs so that electrons have large \hbar and nuclei are doubly dark.

Also non-superconducting neutrinos might be important. The negativity of the neutrino energy in the Z^0 Coulombic fields created by nuclei possessing anomalous weak charge makes possible creation of neutrino-antineutrino pairs from vacuum by the splitting of $\nu\bar{\nu}$ type wormhole contacts with neutrino and antineutrino at causal horizons. Hence the $\nu\bar{\nu}$ wormhole contacts, in particular those of $k = 151$ neutrinos assignable to cell membranes, could be important. Cognitive neutrino pairs indeed play a key role in TGD based model for cognition. The decay of cognitive neutrino pairs to ordi-

nary neutrino-antineutrino pairs followed by a possible transition to dark neutrino phase provides a possible mode of quantum control by creating and controlling the density of super-conducting dark neutrino Bose-Einstein condensates.

The special feature of the cognitive neutrino pairs is that they have nearly vanishing total energy and other quantum numbers. This makes them ideal candidates for realizing Boolean thoughts as sequences of cognitive neutrino pairs with the spin of cognitive antineutrino coding for the two values of the Boolean statement. Quantum model hearing [M6] relies on cognitive neutrino pairs and has been one of the quantitative victories of TGD inspired theory of consciousness and it is interesting to see whether it survives in the new vision.

3.1 The analogy between superconductors of type I and quantum critical superconductors

The original proposal was that bio-systems correspond to superconductors of type I near criticality. What makes super conductors of type I so interesting is that they allow the penetration of metastable magnetic field configurations destroying super-conductivity. Field configurations are cylindrically symmetric in the length scale λ and their cross section has very complicated topology consisting of locally stripe like regions of width of order $\lambda \ll \xi$ [25]. In general, the cross section consists of several disjoint regions and each region is characterized by two integers in TGD [D7]. The magnetic flux obeys a generalized quantization condition [?] of form $\oint (p - 2eA)dl = n2\pi$, where v denotes the velocity field of Cooper pairs and magnetic flux can be smaller than its quantized value.

For superconductors of type I metastability makes the magnetic field structure near critical value of the magnetic field an ideal control tool since the topology of the cross section can be varied easily. This means that both memory dating and simple arithmetic operations are possible since the fusion of two disjoint regions corresponds to the addition of the integers n_1 . This suggests that both the topology of the magnetized region and integers n_1 and/or n_2 code the content of the observation at various p-adic levels. In the absence of sensory input the magnetic field reduces to ground state configuration (no super-conducting regions) with related integers perhaps coding long term memories.

Quantum critical superconductors are naturally superconductors of type II but in this case the supra current carrying regions are associated with the boundaries of dynamical stripe like structures so that the situation remains

more or less unchanged. The super-conducting regions are associated with the boundaries between regions possessing different value of \hbar and stripes correspond to a larger value of \hbar . Wormhole Cooper pairs are at the boundary region of two phases.

The lipid layers of the cell membrane ($k = 149$) and the entire cell membrane itself ($k = 151$) as well as the endoplasmic membranes filling the cell interior indeed resemble locally super-conducting regions of quantum critical super conductor since the thickness of the membrane is very small as compared to its typical radius of curvature. The join along boundaries bonds between cells (identified as the so called gap junctions [26]) could give rise to macroscopic super conductor. In nerve cells axons are long cylindrically symmetric configurations of this type.

In accordance with the magnetic metastability, the endoplasmic membranes of the cell are known to be dynamical structures, which change their size and connectedness continually. An additional support for the role of the superconductivity in the cellular information processing comes from the empirical observation that strong magnetic fields have harmful consequences for the information processing of the cell. Above critical magnetic field vortices of radius ξ inside which large \hbar phase is transformed to ordinary one would be formed. Cell size gives a good estimate for the value of the coherence length ξ of dark neutrino super-conductor identified as weak length scale.

3.2 Empirical guidelines

The empirical guidelines are following.

a) p-Adic mass calculations utilizing the information about neutrino mass squared differences support the view that neutrino Compton length scale is about $L(169)$ and neutrinos have mass of $\sim .2$ eV [F3]. There is evidence for other mass scales too, in particular $L(173)$. p-Adic mass calculations [F4] led to the conclusion that also hadronic quarks can correspond to several p-adic primes, even in the case of low mass hadrons. The TGD based model for nuclear physics assumes that color bonds having $k = 127$ quarks at their ends with MeV mass scale connect nucleons to nuclear strings. These findings encourage to ask whether also Gaussian Mersennes $k = 151, 157, 163, 167$ would define mass scales of neutrinos. The corresponding dark mass scales for $\hbar \rightarrow \hbar/v_0 \simeq 2^{11}\hbar$ correspond to $k_{eff} = 173, 179, 185, 189$ and span the length scale range $20 \mu\text{m}-.5$ cm.

The earlier model of neutrino superconductivity and cognitive neutrino pairs was based on $k = 151$ ordinary neutrinos having long ranged weak

interactions. The new view about long range weak interaction requires much more massive neutrinos having dark Compton length around $L(151)$. Since both electron and nuclear exotic quarks [F8] correspond to Mersenne prime M_{127} , the natural guess is that also neutrinos can exist in $k = 127$ state with electron neutrinos having scaled up .55 MeV rather near to electron mass. A possible explanation for the special role of M_{127} that it is largest Mersenne prime corresponding to a non-super-astrophysical length scale. One can also consider interpretation in terms of almost unbroken electro-weak symmetry for fermions. The corresponding dark length scale would be $L(k_{eff} = 149)$ and would correspond to the thickness of the lipid layer of cell membrane.

b) The model for the anomalies of water [F9] led to the conclusion that one fourth of hydrogen atoms of water are in dark matter phase with large value of \hbar and that hydrogen atoms form linear super nuclei. This hypothesis allows to estimate the Coulombic Z^0 interaction energy of dark neutrinos with water molecules. The large density of anomalous Z^0 charge for doubly dark matter with $L_w \simeq n^3 \times .2 \mu\text{m}$ does not however require neutrino screening since color force can compensate the weak force as discussed in [F9]. The argument below shows that even in $k = 127$ neutrinos effective screening would require relativistic dark neutrinos since the density of dark neutrinos should be roughly one half of the density of water molecules for complete screening and too large by about three orders of magnitude.

c) The model for tritium beta decay anomaly gives the estimate $1/\mu\text{m}^3$ for the density of dark neutrinos in condensed matter. The density could of course be also higher in living matter. The requirement that dark neutrinos are non-relativistic implies strong bound on their density via Fermi momentum. One obtains

$$E_F \ll m_\nu , \quad (1)$$

which by using the expression for E_F gives for effective dimensions $D = 1, 2, 3$ the bounds for $n_{\nu,D}$

$$\begin{aligned} n_{\nu,1} &\ll \frac{1}{\sqrt{2\pi}} \frac{m_\nu}{\hbar} , \\ n_{\nu,2} &\ll \frac{1}{2\pi} \frac{m_\nu^2}{\hbar^2} , \\ n_{\nu,3} &\ll \frac{1}{6\pi^2} \frac{m_\nu^3}{\hbar^3} . \end{aligned} \quad (2)$$

In large \hbar phase the dark neutrino density is scaled down by a large factor. In 1-D case the 3-D density is obtained by dividing by the transversal area S of the linear structure involved. The transversal size scale must at least be of the order of dark neutrino Compton lengths so that only numerical constants distinguish between the 3-D density in various effective dimensions.

Even for $k = 127$ the conditions guaranteing non-relativistic Fermi energy are non-trivial and read as

$$\begin{aligned}
n_{\nu,1} &\ll \sqrt{2}x \frac{1}{L(151)} , \\
n_{\nu,2} &\ll 2\pi x^2 \frac{1}{L^2(151)} , \\
n_{\nu,3} &\ll \frac{8\pi}{6} x^3 \frac{1}{L^3(151)} , \\
x &\simeq 11.3 .
\end{aligned} \tag{3}$$

The order of magnitude is few neutrinos per nm length scale which means that dark neutrino Cooper pairs with minimum size $L(151)$ have overlap which makes Bose-Einstein condensation possible. The upper bound for the density of Cooper pairs is considerably lower than the density of dark hydrogen nuclei if 1/4:th of hydrogen nuclei are in doubly dark phase: the ratio of 3-D densities is smaller than $(5.7, 8, 60) \times 10^{-4}$ for $D = 1, 2, 3$ if 1/4:th of hydrogen atoms are in dark phase and if all dark hydrogen atoms make a phase transition into a doubly dark phase in a given region. Therefore dark neutrinos cannot screen anomalous weak charge. Neutrino screening is not needed since long range color forces can compensate the repulsive weak force.

For $k \geq 151$ situation the conditions guaranteing non-relativistic Fermi momentum cannot be satisfied for dark neutrino density $\sim 1/\mu m^3$. Hence the conclusion seems to be that $k \geq 151$ dark neutrinos are most naturally relativistic.

d) Z^0 force is automatically vacuum screened above length scale L_w , which is about 3 – 6 Angstroms for dark nuclear matter with $n = 3$ and 1.8 – 3.6 μm for doubly dark case. In the latter case the screening condition does not pose condition on neutrino density. For $k \geq 151$ the condition implies that dark neutrinos are relativistic.

Z^0 magnetic penetration length λ_Z is obviously not longer than L_w . If there is active screening by supra currents one has $\lambda_Z < L_w$. This gives using $\lambda^2 = m_\nu/4\pi g_Z^2 n_c$

$$\begin{aligned}
n_{\nu,1} &> m_{\nu}L_w \times \frac{S}{4\pi g_Z^2 L_w^2} \frac{1}{L_w} , \\
n_{\nu,2} &> m_{\nu}L_w \times \frac{d}{4\pi g_Z^2 L_w} \frac{1}{L_w^2} , \\
n_{\nu,3} &> m_{\nu}L_w \times \frac{1}{4\pi g_Z^2 L_w^3}
\end{aligned} \tag{4}$$

Here S *resp.* d is the transversal area *resp.* thickness of effectively 1-D *resp.* 2-D super conductor. Notice that this conditions does not involve \hbar at all and it seems that the large value of \hbar automatically implies that L_w gives the magnetic penetration length. For $k = 151$ the 3-dimensional densities are in all cases of order few neutrinos per $L^3(151)$ so that the together with the conditions guaranteing non-relativistic Fermi energy these conditions force dark neutrino density to a rather narrow range. For $d = L(151)$ and $S = L(151)^2$ the lower bound for 3-D density is same in all cases and given by $n_{\nu,3} > .3/L(151)^3$ for $m(\nu_e) = .55$ MeV. The lower bound is by three orders of magnitude below the upper bound from the requirement that situation is non-relativistic. The upper bound for the 3-D density give the rough lower bound $\lambda > 10^{-3/2}L_w \simeq 6L(151) > \xi_T \simeq L(151)$, where ξ_T is estimate for the transversal coherence length so that in the transversal direction type II superconductor would be in question. In longitudinal direction the coherence length $\xi_L = L_w > \lambda$ identified as a length of Cooper pair flux tube structure would mean type I super conductivity. The interpretation could be as follows. If axonal membrane is this kind of mixed superconductor, overcritical Z^0 magnetic field parallel to axon, would penetrate in flux quanta parallel to axon. For type I case transversal Z^0 magnetic field near criticality would penetrate into the axonal membrane as stripe like patterns with stripes of width λ .

The Compton length of neutrino gives lower bound for the thickness of the magnetic flux tube of the dark neutrino Cooper pairs.

a) $L(149)$ and $L(151)$ would correspond to lower bounds for thickness and length of the flux tubes for dark $k = 127$ neutrinos. In effectively 1-D case $k = 127$ with $S = L^2(149)$ neutrinos give for the neutrino density a lower bound which is of order one neutrino per $1/\mu m$. This would suggest that the lipid layers of cell membrane correspond to the pair of magnetic flux tubes defining the wormholy neutrino Cooper pairs.

b) One can also consider the possibility that the height of Cooper pairs is scaled up to $L(k_{eff} = 151 + 22) = L(173) = 20 \mu m$ would give the length

of the flux tube and axons between cell membranes are good candidates here. The vacuum screening of weak interaction above L_w however strongly suggests $\xi < L_w$.

3.3 Dark neutrino superconductor as a quantum critical superconductor

The scarcity of the empirical guide lines forces the use of the model of quantum critical electronic superconductivity as the basic format. For $k = 127$ neutrinos the generalization of the wormhole model for electron Cooper pairs is not completely straightforward task since the finite range $L_w \simeq n^3 \times .2 \mu\text{m}$ of exotic weak interactions causes delicacies.

3.3.1 The case of $k = 127$ neutrinos

The following arguments fix the generalization of the model for dark neutrino Cooper pairs in the case of $k = 127$ neutrinos.

a) Since the relevant length and mass scales of neutrinos and electrons are essentially identical, the dark neutrino Cooper pairs are expected to have similar sizes and are both associated with the boundaries between doubly dark and ordinary nuclear matter. In the case of cell interior and exterior would naturally correspond to these phases of matter. Of course, only partial darkness is possible: the model explaining the anomalies of water [F9] suggests that 1/4:th of hydrogen ions is in doubly dark phase in the cell interior and in dark phase in cell exterior.

b) The model of ORMES as superconductors assumes that dark electrons have large \hbar with $k_{eff} = 149$ and nuclei are in doubly dark phase with $k = 127$ dark quarks coupling to doubly dark $k = 113$ weak bosons possessing range of order $L_w \simeq n^3 \times .2 \mu\text{m}$. The wormhole Cooper pairs of dark electrons and neutrinos can be assumed to have same transversal size $L(149)$ as ordinary Cooper pairs.

c) The expression for the energy of Cooper pair has the general form $E = a/L^2 - b/L$ corresponding to kinetic energy and Coulombic interaction energy. The scaling up of \hbar in the stability condition of for Cooper pairs discussed in [J1] amplifies the contribution of the kinetic energy by a factor 2^{22} . This means that this factor also scales up the length of the Cooper pair to about 4 cm.

The situation is not quite this simple however. The most obvious implications of the finite range of the exotic weak force are $\lambda \simeq L_w$ and $\xi \leq L_w$, which is rather near to $L(167) = 2.5 \mu\text{m}$ for $n = 3$. It simply does not make

sense to talk about coherence and correlations above the weak length scale L_w . Therefore the energy of the Cooper pair is minimized subject to the constraint $L \leq L_w$ for the length of the Cooper pair which gives $L = L_w$. Situation remains the same even in the case of triply dark nuclear matter giving $L_w = n^3 \times .4$ mm.

Cell membranes and the dynamical endoplasmic membranes within cell have interpretation as stripe like regions to which super-conducting dark electrons and neutrinos can be associated naturally. Macroscopic quantum coherence is often assigned to the ordered water in cell interior and the question is whether ordered water could correspond to doubly dark phase. One can also wonder whether the phase transitions between sol and gel phases associated with nerve pulse activity could correspond to transitions between dark and doubly dark phases. Since the transversal length scale of chromosomes and micro-tubules is also characterized by $L(151)$, it is natural to expect that dark electrons and neutrinos play key role in the dynamics of these structures.

3.3.2 Is neutrino superconductivity possible for $k \geq 151$?

For $k \geq 151$ the doubly dark coherence lengths are much longer than L_w for doubly dark matter. One would however expect that the coherence length for Cooper pairs should be longer than the Compton length. Situation changes if dark nuclei correspond to triply dark nuclei with $L_w \simeq 3.6$ mm for $n = 3$ triply dark nuclei. The requirement that coherence length is longer than Compton length is satisfied up to $k = 157$ and for $k = 163, 167$ L_w defines naturally the height of Cooper pair space-time sheet.

By the naive scaling the radius of the flux tube associated with neutrino Cooper pair would be $L(k + 22)$, $k = 151, 157, 163, 167$. The naive scaling of $L(151)$ giving the height of the flux tube would give for the height of neutrino Cooper pair $L(k + 44)$ which is longer than L_w for triply dark matter. As in the previous case L_w would be the upper bound for the height and would correspond to a maximal binding energy. These length scales would determine the transversal and longitudinal coherence lengths ξ_T and ξ_L of neutrino superconductor.

As already found, it is not possible to have non-relativistic Cooper pairs for reasonable values of dark neutrino density. Also stability condition assuming non-relativistic dark neutrinos leads to contradiction. Hence the energy of neutrino is difference of relativistic energy $E = 2\pi/L$ and Z^0 Coulombic interaction energy behaving in the same manner with respect to scalings. This implies that minimum energy is achieved for $L = L_w$. The

scale of zero point kinetic energy would be $E = 2\pi/L_w \simeq E = 3.4$ K.

Unless ordinary and dark space-time sheets are thermally isolated, the BE condensate is thermally unstable for $k > 151$. For $k = 151$ dark neutrinos the critical temperature determined by $E_0 \sim 2\pi/L(151) \simeq 800$ K and gives critical temperature of order room temperature. Thermal isolation in reasonable time scales might be however possible since only de-coherence phase transition mediates interactions between ordinary matter and dark neutrinos.

The large values of these scales would mean that dark neutrino superconductivity would relate to the control of smaller structures of size of order neutrino Compton length $\sim L(k)$ by structures of size $L(k + 22)$. The de-coherence transition in which dark neutrino Cooper pairs decay to ordinary neutrinos would certainly be an essential aspect of this transition. The creation of ordinary neutrinos by the splitting of $\nu\bar{\nu}$ wormhole contacts (cognitive neutrino pairs) would be another facet of the quantum control.

3.4 Structure of brain and neutrino super conductivity

The structure of the brain affords evidence for the p-adic hierarchy of superconductor structures associated with coherence lengths ξ and suggests that sensory stimulus represents itself regions of larger \hbar at various levels of the condensate containing cells activated by the sensory stimulus. Regions carrying magnetic fields could correspond to both the weak magnetic fields guaranteeing effective one-dimensionality of the super conductor or magnetic fields associated with the defects of the super conductor.

Perhaps the entire organism could be regarded as a hierarchy of quantum critical superconductors with superconducting regions identifiable as boundaries between regions having different values of \hbar : the larger the structure the larger the value of \hbar . The radius of curvature of cell membrane is so large that locally the magnetic field has constant direction.

In the absence of sensory input the condensate levels carry some preferred magnetic field configuration. The simplest possibility is the presence of constant magnetic or Z^0 magnetic field. The magnetic field of the flux tube containing the Bose-Einstein condensate of wormhole Cooper pairs does not destroy the superconductivity based on spin 1 Cooper pairs. Topological field quanta are quite generally characterized by frequency type parameters ω_1, ω_2 and integers n_1, n_2 assignable to the increments of phases of CP_2 complex CP_2 coordinates around homologically nontrivial loops and analogous to angular momentum values [D7]. In particular, the integers n_1 could be carrier of biologically relevant information.

A fascinating possibility is that the Gaussian and ordinary Mersennes associated with $k = 113, 127, 151, 163, 167$ define the fundamental p-adic length scales and the large \hbar satellites of these length scales could give rise fractal copies of the structures in these length scales scaled up by powers of $n/v_0 \simeq n \times 2^{11}$. In particular, the Mersennes $k = 127, 151, 157, 163, 167$ span 40 half octaves whereas the Mersennes 89, 107, 113, 127 span 39 half octaves. Therefore one can wonder whether the biologically most relevant length scale range could contain a scaled down copy of elementary particle physics such that $k = 167, 163, 157$ correspond to three charged lepton generations.

Be as it may, the two lowest levels in the dark hierarchy cover the length scales associated with living organisms. Second fascinating possibility is that the twin primes $k, k + 2$ might be of special biological relevance as the appearance of various twin structures in bio-matter would suggest. In the following the empirical evidence supporting these hypothesis is discussed.

3.4.1 Structures in the cell length scale, miracle length scales, and twin primes

The miracle length scales defined by Gaussian Mersennes should make themselves manifest in cell length scales.

a) The two-layered structure of the cell membrane and of endoplasmic membranes would naturally correspond to $k = 149$ and $k = 151$ p-adic levels. Membranes could be identified as regions between large \hbar phase in the interior of cell and ordinary phase in the exterior of cell carrying wormhole Cooper pairs of electronic and neutrino type quantum critical superconductors and containing also cognitive neutrino pairs.

b) The interior of the cell contains structures, which might be identified with condensate levels $k = 163$ and $k = 167$, and might correspond to some higher levels in the information processing hierarchy of the cell. Cell nucleus with size in the range $5 - 10 \mu\text{m}$ can accommodate all the miracle length scales. Biophotons [15] have energies in visible range and ultraviolet and visible wavelengths thus almost cover miracle length scales. For large \hbar variants the wavelengths would be scaled up by powers of n/v_0 and these photons might be involved with quantum control of short length scales by longer length scales. The formation of Bose-Einstein type condensate of bio-photons could relate to the formation of gap junctions between cells.

c) The next level corresponds to a pair of length scales $L(167) = 2.5 \mu\text{m}$ (lower bound for the cell size) and $L(169 = 13^2) = 5 \mu\text{m}$ allowed if one generalizes length scale hypothesis so that it allows k to be power of prime. The size of cell nucleus varies in the range $5-10 \mu$ and one can wonder

whether this length scale pair and corresponding Cooper pairs could relate to the twin structures formed by chromosomes and to the doubling of DNA during cell division.

d) Epithelial sheets consist of double cell layers and appear very frequently in multicellular bio-systems (skin, glands, sensory organs, etc.). It would be natural to interpret them as region in large \hbar phases can be present. Eye provides an example of this kind of structure [26]: eye can be regarded as a composite structure consisting of single cell layer (rods and cones) and two-layered structure consisting of layers of bipolar cells and ganglion cells. Great variety of super-conductors are possible at this length scale. These structures might involve doubly dark neutrino and electron super conductivity with transversal length scales $L(149 + 22) = L(171) = 10 \mu\text{m}$ and $L(151 + 22) = L(173) = 20 \mu\text{m}$.

3.4.2 Scaled up variants of cell membrane?

The information processing of the brain could involve dynamical membrane like structures inside the brain as dynamical units with electron and neutrino super-conductivity playing key role in the functioning of the structure. This would mean that the couplings between cells of the brain understood as neural net should have tendency to form dynamical two-dimensional surface like structures.

These higher level membranes could have functions analogous to those of ordinary cell membranes. Action potential between the cell layers and nerve pulse might be well defined concepts. These membranes could form cell like structures filled with dynamic "endoplasmic" membranes. For instance, the twin primes $k = 179, 181$ could define generalized cell membrane like structure of thickness $L(181) \simeq 320 \mu\text{m}$.

Generalizing the ideas of TGD one might speculate that these membranes could act as Josephson junctions and communication between the structures should take place via counterparts of ordinary nerve pulses: also the existence of the counterpart of EEG is suggestive. Various parameters characterizing exotic nerve pulse and EEG should be related by simple scaling to those characterizing ordinary nerve pulse and EEG.

3.4.3 Cortical structures and first level satellites of miracle length scales

The obvious place for the identification of large scale super conducting structures of is cortex. The relatively small thickness of the cortex (about 1 mm)

implies that curvature effects do not mask the local cylindrical symmetry. Cortex is indeed known to possess columnar organization. For instance, in visual cortex there are two columnar structures with very complicated cross section perhaps identifiable as stipe like structures associated with quantum critical super-conductivity at higher level of dark matter hierarchy. These structures have also binary structure characteristic for the wormholy Cooper pairs.

1. Field axis orientation columns

The first columnar structure [26] in the visual cortex corresponds to the so called field axis orientation columns consisting of locally stripe like regions of cells (see Fig. 3.4.4), which preferentially react to the orientation of a bar of light in the visual field. The width of the stripes with fixed orientation is about $20 - 50 \mu\text{m}$ [26].

The first large \hbar satellite of $L(151)$ is indeed $L(173) = 20 \mu\text{m}$. A possible interpretation is that continued stimulus with fixed orientation creates at $k = 173$ level a cylindrical magnetic field configuration, which leaves only the regions reacting to this particular orientation in super conducting state. Doubly dark electronic and neutrino super conductors for which the length scales corresponding to $k = 171$ and 173 would appear naturally in the large \hbar scaling of the cell membrane. It should be noticed that $k = 171$ corresponds to the upper bound $10 \mu\text{m}$ for the size of nucleus varying in the range $5-10 \mu\text{m}$.

Ocular dominance columns

Ocular dominance regions consist of cells reacting appreciably to the stimulus from the second eye only, and form columnar structures [26] with complicated cross section and become visible via a continued stimulation of one eye only (see Fig. 3.4.4). The typical width of the stripe in the region is about $200 - 500 \mu\text{m}$.

The weak length scale of triply dark nuclear matter corresponds to $k_{eff} = n^3 \times 400 \mu\text{m}$ so that $n = 1$ would make sense. The large \hbar satellite of $L(157)$ is $160 \mu\text{m}$.

The levels $k = 179$ and $k = 181$ forming a pair with $L(179) \simeq 160 \mu\text{m}$ might be the relevant p-adic levels now. The ocular dominance columns associated with right and left eye alternate and the regions formed by right-left pairs of ocular dominance columns is a natural candidate for the double layered structure at level 179 involving Bose-Einstein condensate of wormholy Cooper pairs.

3. Hyper columns

The visual cortex contains also larger structures, "hyper columns" [26], which form basic units for the processing of visual information (and sensory information in general). These structures have roughly the size of order 1 mm, the thickness of the cortex. The large \hbar satellite of $L(163)$ is 1.28 mm. $L(167)$ would give to large \hbar satellite $L(167 + 22) = L(189) = .5$ cm. Also structures with this size scale could also appear in brain.

3.4.4 Structures in the length scale of body and second level satellites of miracle length scales

In contrast to the prevailing view in neuroscience, in TGD framework entire body is seat of consciousness and brain only builds symbolic representations about sensory data. Also the idea about body as a passive receiver of commands from brain is given up and brain and body can be said to react to the desires of the magnetic body serving as a space-time correlate for the intentional me. Hence it makes sense to consider the possibility that also structures with scales larger than typical brain structures could be of importance for understanding conscious experience and functioning of living system.

The higher large \hbar satellites of $k = 151, 157, 163, 167$ are $k = 195, 201, 207, 211$ and correspond to length scales 4 cm, 32 cm, 2.5 m, 10 m. $k=163$ and 167 could correspond to quantum critical super-conductivity in large sized organisms. These length scales could be also important for the structural organization of bio-systems. The fourth level in the hierarchy of dark nuclear matters would correspond to $L_w = n^4 \times .8$ m and might have relevance for information processing in the length scale of human body.

Double layered structures (both k and $k + 2$ primes) might appear in these length length scales.

a) For $k = 191, 193$ one has $L(191) \simeq 1$ cm.

b) $k = 197, 199$ is the largest doublet, which might be realized in bio-systems one has $L(197) \simeq 8$ cm. One cannot exclude the possibility that right and left brain hemispheres correspond to the condensation level $k = 197$ and whole brain to the condensation level $k = 199$.

c) For the next pair ($k = 227, 229$) (note the large gap in development) one has $L(227) \simeq 2500$ m, which is probably not realized in bio-systems at the level of organisms. One can of course ask whether biological organisms could form super organisms involving these higher levels.

3.5 Cognitive neutrino pairs

The notion of cognitive neutrino pairs seems to survive the new interpretation of long range weak gauge fields although dramatic modifications of the model are necessary.

3.5.1 Cognitive neutrino pairs as $\nu\bar{\nu}$ wormhole contacts

Cognitive neutrino pairs can be identified as $\nu\bar{\nu}$ wormhole contacts. The throat carrying antineutrino quantum numbers would be at the space-time sheet carrying oxygen and ordinary hydrogen atoms so that $\bar{\nu}$ throat would experience only the ordinary weak force. The throat carrying neutrino quantum numbers would be at the space-time sheet of dark or doubly dark hydrogen ions. This would imply large negative weak interaction energy with the hydrogen ions which can be even larger than the mass of the neutrino. Hence the generation of cognitive neutrino pairs would be energetically favored and the splitting of the wormhole contacts could produce ordinary $k = 127$ antineutrinos and dark $k = 127$ neutrinos. The latter could in turn form Cooper pairs of dark neutrino super conductor.

The repulsive interaction between dark neutrinos and the weak screening caused by them implies that some maximum number of them can be generated (note that the compensation of weak force by color force allows net weak charge). This means that cognitive neutrino pairs, besides serving in the role of bits arranged along linear structures defined by the stripes of doubly dark water ions, could also perform bio-control.

In a good approximation the mass of the cognitive antineutrino is obtained by scaling up the mass of ordinary $k = 169$ neutrino by a factor $2^{(169-127)/2} = 2^{21}$. Using the results of p-adic mass calculations [F3] this gives the estimates

$$\begin{aligned}
 m(\nu, 127) &= \frac{L(169)}{L(127)}m(\nu_\mu, 169) = 2^{21}m(\nu_\mu, 169) \ , \\
 m(\bar{\nu}_\mu, 127) &= m(\bar{\nu}_\tau, 127) \simeq 1.47 \text{ MeV} \ , \\
 m(\bar{\nu}_e, 127) &\simeq .55 \text{ MeV} \ .
 \end{aligned}
 \tag{5}$$

For $k = 127$ electron neutrinos mass is about .55 MeV.

The Z^0 Coulombic interaction energy of dark $k = 127$ neutrino with water molecule is obtained by integrating the Coulomb potential energies with hydrogen ions carrying anomalous Z^0 charge for a stripe stripe of length

$L_w \simeq n^2 \times .2 \mu\text{m}$ containing doubly dark hydrogen ions. The expression for the interaction energy is given by

$$\begin{aligned} E &= \int_0^{L_w} V_Z(\nu, p) n dz dS , \\ V_Z &= \alpha_Z Q_Z(\nu) Q_Z(p) \frac{z - L_w}{S} , \\ n &\simeq \frac{1}{2} n_{H_2O} \simeq \frac{1}{2} \times \frac{1}{18a^3} , \end{aligned} \quad (6)$$

where S is the transversal area of the stripe, n_{H_2O} is the number density of water molecules, $Q_Z(p)$ is the anomalous Z^0 charge assignable to proton: twice the Z^0 charge of neutrino, and $a = 0.1 \text{ nm}$ is natural unit of length.

This gives

$$\begin{aligned} E &= \frac{1}{72} \alpha_Z Q_Z(\nu) Q_Z(p) \left(\frac{L_w}{a}\right)^2 \times \frac{1}{a} , \\ \alpha_Z &= \frac{\alpha_{em}}{\sin(\theta_W) \cos(\theta_W)} , \quad Q_Z(\nu) = \frac{1}{4} + \sin^2(\theta_W) , \quad Q_Z(p) = -2Q_Z(\nu) , \\ L_w &= n \times 2 \times 10^3 a . \end{aligned} \quad (7)$$

For $n = 1$ one obtains the estimate $E = .76 \text{ MeV}$ which is smaller than the estimate $M_w = 2m_{\nu_e} = 1.1 \text{ MeV}$ for the mass of $\nu_e \bar{\nu}_e$ wormhole contact. For μ and τ neutrinos one would have $M_w = 2m_{\nu_\mu} = 2.9 \text{ MeV}$. For $n = 3$ the formula gives 6.5 MeV . Therefore the generation of cognitive neutrino pairs should occur spontaneously for $n = 3$ and for electronic neutrinos perhaps also for $n = 1$.

One can also consider the possibility wormhole contacts for which throats correspond to $k = 151$ exotic neutrinos coupling to W bosons with $L_w = n \times a$. Electron neutrino is estimated to have mass 138 eV . In this case the average binding energy would be

$$E = \frac{n^3}{36} \alpha_Z Q_Z(\nu) Q_Z(p) \frac{1}{a} . \quad (8)$$

$n = 1$ gives $E = .44 \text{ eV}$, which happens to belong to the energy range metabolic energy quantum whereas $n = 3$ gives $E = 3.9 \text{ eV}$. Spontaneously occurring generation of wormhole contacts is not favored in this case.

3.5.2 Model for the generation of cognitive neutrino pairs

The generation of cognitive neutrino pairs is a purely TGD based phenomenon made possible by the large binding energy of $k = 127$ dark neutrinos in condensed matter which is much larger than neutrino rest mass. This makes possible a process in which neutrino-antineutrino pair having negative total energy and other quantum numbers is generated by the splitting of $\nu\bar{\nu}$ wormhole contact connecting the space-time sheet containing ordinary nuclei of water molecules and the space-time sheet containing doubly dark hydrogen ions. Antineutrino is assumed to correspond to the throat at the ordinary space-time sheet and neutrino to the throat at doubly dark space-time sheet. The splitting of the wormhole contact gives rise to neutrino antineutrino pair and dark neutrinos could in turn form Cooper pairs so that the generation of wormhole contacts could serve control purpose.

$\nu\bar{\nu}$ wormhole contact defines a cognitive neutrino pair in the sense that dark neutrino spin defines naturally a representation of bit. The spin of cognitive neutrino pairs can be flipped if the space-time sheet of dark neutrinos contains dynamical Z^0 magnetic field.

One can also consider the possibility that cell membrane represents double sheeted cognitive structure, 'wormhole magnetic field', glued to the outer boundary of cell, and that Z^0 magnetic field is generated by rotating Z^0 wormhole contacts [J5]. The conservation of Z^0 magnetic flux might however contradict the assumption that Z^0 fields are short ranged at the space-time sheet of ordinary atoms. The required magnetic field must be rather strong and cell membrane provides an excellent candidate for the regions at which cognitive neutrino pairs are created. The large value of \hbar also increases the size of magnetic flux quantum by a factor 2^{11} .

3.5.3 Relativistic and non-relativistic cognitive neutrino pairs

There are two options concerning the modelling of cognitive neutrinos corresponding to relativistic and non-relativistic situations. At the relativistic limit the expressions for energies of the states

$$\begin{aligned}\omega(n+1, up) &= \sqrt{2n - \Delta g/2} \sqrt{Q_Z(\nu) g_Z B_Z} , \\ \omega(n, down) &= \sqrt{2n + \Delta g/2} \sqrt{Q_Z(\nu) g_Z B_Z} .\end{aligned}\tag{9}$$

where Δg represents anomalous Z^0 magnetic moment of dark neutrino which is extremely small but crucial in the model of hearing [M6]. For the considerations to follow the value of Δg does not matter.

For the second option cognitive neutrino is non-relativistic (classically this guarantees that cognitive antineutrino does not escape from the system) and the energies are given by

$$\begin{aligned}
\omega(n+1, up) &= (n - \frac{\Delta g}{4})\omega_c , \\
\omega(n, down) &= (n + \frac{\Delta g}{4})\omega_c , \\
\omega_c &= \frac{Q_Z(\nu)g_Z B_Z}{m(\bar{\nu})} .
\end{aligned} \tag{10}$$

The very low frequency associated with the transition $\omega(n+1, up) \leftrightarrow \omega(n, down) = \frac{\Delta g \omega_c}{2}$ codes for audible frequencies in the model of hearing [M6].

3.5.4 Quantization of the Z^0 magnetic flux

Quantization of the Z^0 magnetic flux applied to the cylindrical shell defined by the axonal cell membrane gives the constraint

$$\begin{aligned}
2Q_Z(L)g_Z B_Z &= \frac{k\hbar}{dR} , \\
Q_Z(L) &= \frac{1}{4} - \sin^2(\theta_W) \simeq .02 .
\end{aligned} \tag{11}$$

$k = 1$ is the minimum value of the integer k . $d \simeq L(151)$ denotes the thickness of the cell membrane and R is the radius of the axon. Here the electronic Z^0 charge of $Q_Z(L)$ must be used. The requirement that flux quantization condition holds also true for the Cooper pairs of neutrinos implies the the ratio of corresponding Z^0 charges is integer: this gives

$$\frac{Q_Z(\nu)}{Q_Z(L)} = \frac{\frac{1}{4} + \sin^2(\theta_W)}{\frac{1}{4} - \sin^2(\theta_W)} = n . \tag{12}$$

This condition allows infinite number of solutions

$$\sin^2(\theta_W) = \frac{k}{4k+1} , \quad k = 0, 1, 2, \dots . \tag{13}$$

varying in the range $(0, 1/4)$. For $k = 3$ one has

$$\sin^2(\theta_W) = \frac{3}{13} \simeq .23072 . \quad (14)$$

It deserves to be noted that the solution is equivalent with the condition $4\sin^2(\theta_W) = 24/26$: rather amusingly, the basic dimensions of bosonic string model appear in this expression. Not only amusingly, this value is consistent with the high precision value of Weinberg angle $\sin^2(\theta_W) = .2294 \pm .001$ measured in 1994 by K. Abe and collaboration [27].

If $2Q_Z(L)$ as unit of Z^0 magnetic flux, the resulting unit of magnetic flux is by a factor 25 larger than when $2Q_Z(\nu)$ is used as unit. The weakest possible Z^0 magnetic field has strength of about $.5 \times 10^{-4}$ Tesla (strength of Earth's magnetic field) for $2Q_Z(\nu)$ option whereas for $2Q_Z(L)$ option this field has strength of about $.25 \times 10^{-2}$ Tesla.

The unit of quantization increases by a factor $\simeq 2^{11}$ if neutrino is in large \hbar phase. This scales up the value of the magnetic transition energy scale $E = \hbar\omega_c$ by a factor $\simeq 2^{22}$. For electron neutrino with mass .55 MeV and $2Q_Z(\nu)$ as a unit this scale is predicted to be 90 K which is below room temperature. For $2Q_Z(L)$ as unit the scale is .45 eV which corresponds to the metabolic energy quantum.

3.5.5 Does the quantum model of hearing survive the new interpretation of long ranged weak fields?

Cyclotron frequency scales down by a factor 1/2 in the transition ($k = 151 \rightarrow 127, \hbar \rightarrow 2^{11}\hbar$) for neutrinos so that the cyclotron frequency scale is preserved. This does not yet guarantee that the earlier quantum model for hearing relying crucially on the scale $\Delta g \times \omega_c$ survives. The proportionality $\Delta g \propto \alpha_Z m_\nu m_\tau / m_W^2$ [M6] with ν, τ and W referring now to the exotic counterparts of these particles means that Δg does not automatically remain invariant in the transition from standard weak physics to exotic weak physics. The loss of quantum model for hearing would be highly regrettable since it has been one of the basic quantitative victories of TGD inspired theory of consciousness.

One might of course hope that the universality suggested by quantum criticality could imply the approximate invariance of Δg . The transition $k = 89 \rightarrow 113$ for W [$L_w = L(k_{eff} = 113 + 44)$] means the scaling of W mass by a factor 2^{-12} . Taking into account that $\alpha_Z m_\nu / m_W^2$ gives a scaling factor $2^{-11+12+24} = 2^{25}$, the invariance of Δg requires $k_\tau = 107 + 50 = 157$.

This lends support to the speculative idea that the exotic charged leptons (e, μ, τ) could correspond to Gaussian Mersennes (167, 163, 157) in analogy

with the Mersenne hierarchy (127, 113, 107) for the ordinary charged leptons. $k_{eff} = 107 + 44 = 151$ corresponds to doubly dark hadronic space-time sheet and exotic QCD. As in the case of ordinary hadrons also quarks would correspond to these length scales with $k = 167$ defining the counterpart of exotic $k = 127$ quark. The $k = 167$ exotic electron would have mass .5 eV: the miraculous metabolic energy unit pops up again and again.

What looks admittedly strange is that exotic neutrino mass scale would be higher than the mass scale of exotic charged leptons. Somehow it seems that the actual p-adic length scale of exotic neutrino must be longer than $L(167)$.

a) There exists experimental evidence for several scaled up variants of ordinary neutrinos but a convincing picture about the nature of the process changing neutrino mass scale is lacking. For instance, ordinary neutrinos emitted in weak interaction vertices could correspond to the p-adic length scale M_{89} of weak bosons and have p-adic temperature $T_p = 1/2$ implying that the neutrino corresponds effectively to the p-adic length $L(2 \times 89 = 178)$ and mass scale 10^{-2} eV. The size of the space-time sheet of the emitted neutrino could be reduced in a process analogous to de-coherence. The increase of the p-adic prime in this process would force p-adic heating increasing the p-adic temperature of neutrino to $T_p = 1$. The reduction of the size of an exotic neutrino [characterized by even longer p-adic length scale than $L(k_{eff} = 178)$] to $L(127)$ does not however look plausible.

b) The understanding of the mass scale could come from quite different direction. There is evidence for leptohadron physics for which colored excitations of charged leptons give rise to color bound states [F7]. Colored excitations of leptons could correspond to the presence of $k = 127$ dark quark pairs inside leptons of lepton making them color octets. This would be completely analogous to their appearance at the ends of color bonds connecting nucleons to nuclear strings in the model of atomic nucleus [F8]. An interesting possibility is that the $k = 127$ quarks associated with the ends of the color bonds connecting neutrino space-time sheets increases the mass scale of much more lighter exotic neutrino to $k = 127$. Also the electrons associated with lepto-pions could correspond to $k = 167$ mass scale.

3.5.6 $\nu\bar{\nu}$ wormhole contacts as a source of the Z^0 magnetic field?

Z^0 magnetic field must be generated by some mechanism. In the case of wormholy Cooper pairs the magnetic flux could flow between homological magnetic monopoles at the ends of the flux tubes defining the Cooper pair. In recent case lipid layers of the cell membrane would carry the magnetic

fluxes in question.

Second possibility is that the Z^0 current creating the Z^0 magnetic field is a surface current flowing at the boundaries of the space-time sheet of the lipid layer. The magnitude of the surface current measured using g_Z as unit is from Maxwell equations

$$K = \frac{\hbar k}{Rd} . \quad (15)$$

k is the integer appearing in the previous conditions for the quantization of magnetic flux and equals to $k = 1$ by previous argument.

K could correspond to the surface currents of rotating $\nu\bar{\nu}$ wormhole contacts. The directions of rotation on the two sides of membrane should be opposite. In this case one has

$$K = n\beta\hbar = \frac{\hbar}{Rd} ,$$

where n is surface density of neutrinos and β is the rotation velocity of the wormhole contact behaving like neutrino at the dark neutrino space-time sheet. This gives

$$n_2 = \frac{\hbar}{Rd\beta} .$$

The value of the velocity should be small and this gives lower bound $n \gg \hbar/Rd$ for the surface density of wormhole contacts. The lower bound for the average density of cognitive antineutrinos in the axonal volume is

$$n_3 = \frac{2\hbar}{R^2d} \sim 8 \times 10^2 \frac{\hbar}{L(169)^3}$$

for $R = L(169)$.

4 Atmospheric phenomena and super-conductivity

There is a lot of evidence that various electromagnetic time scales associated with the atmospheric phenomena correspond to those associated with brain functioning. If magnetic sensory canvas hypothesis holds true, this is just what is expected. In this section these phenomena are considered in more detail with the aim being to build as concrete as possible vision about the dynamics involving the dark matter Bose-Einstein condensates at super-conducting magnetic and Z^0 magnetic flux quanta.

4.1 Tornadoes as a macroscopic quantum phenomenon involving Z^0 super-conductivity?

Tornadoes represent a piece of not completely understood atmospheric physics. To mention just two questions which have received no satisfactory answer.

a) What makes possible the ability of tornado to preserve its structure and coherence?

b) What makes possible the coherent rotation of matter inside tornado?

c) How to understand various luminous phenomena associated with the tornadoes [35, 36, 37]?

Classical Z^0 forces and the vision about Z^0 magnetic flux tubes as Z^0 super-conductors suggests a new approach to the physics of tornadoes possibly providing also answers to these questions. The ideas about tornadoes have evolved in three steps: tornadoes as Z^0 magnetic spiral vortices, tornadoes as magnetic of Z^0 magnetic analogs of a rotating magnetic system known as Searl device, and tornado as a system corresponds to scaled up dark matter variant of cell like structure. These approaches, probably not mutually consistent in every detail, will be discussed in the following.

4.1.1 Tornadoes as Z^0 magnetic spiral vortices?

The basic idea is that tornadoes are a phenomenon involving complex many-sheeted space-time topology and classical Z^0 magnetic fields in an essential manner making tornadoes also macroscopic quantum systems in meteorological length and time scales.

a) A partial answer to the question relating to the stability and coherence is self-organization, which in fact implies in TGD context that tornado has 'self' and is conscious in some primitive sense. In standard physics context the ability of tornado to have a well defined macroscopic structure despite the locally chaotic nature of the hydrodynamic flow involved, is not easy to understand. In particular, self-organization does not as such explain the coherent rotation of the matter inside tornado.

b) In TGD framework the answer to the question relating to the rotation of matter inside tornado is that tornado corresponds to Z^0 magnetic flux tube or more generally a more complex structure consisting of Z^0 magnetic flux quanta, say flux walls.

This implies that ions rotate with almost the same rotation velocity in same direction in the Z^0 magnetic field associated with the space-time sheet of the tornado. Although rotation velocities can have both signs, coherent motion in single direction can occur stably. Z^0 magnetic field is generated if

all neutrinos do not co-rotate with the matter or if the screening of nuclear Z^0 charge by neutrinos is not complete. Conducting and super-conducting neutrinos are expected to be unable to follow the rotation of the nuclei whereas the neutrinos below Fermi surface should co-rotate with matter so that Z^0 magnetic field can be generated. Situation is completely analogous to that of an electric conductor.

c) The quantization of Z^0 magnetic field of tornado to flux tubes structures suggests strongly itself and classical orbits of Z^0 charges in average Z^0 magnetic field correspond to Z^0 magnetic flux tubes with helical shape. In case of tornado these flux tubes are expected to have spiral like structure implied by garden hose instability and provide an example of spiral waves which seem to be a very general phenomenon in excitable media. Just like the flux tubes of the magnetic field, also Z^0 magnetic flux tubes are expected to be super-conducting.

d) The mechanism for the breaking of the ordinary super-conductivity in case of the magnetic flux tubes is based on the idea that for curved flux tubes ionic current with an overcritical ion velocity leaks along join along boundaries bonds from the magnetic flux tubes to non-super-conducting space-time sheets. The reason is simply the inertia of the charged particle. This process implies the generation radiation in case of the ordinary electromagnetic ions. This process occurs in the reconnection of magnetic flux tubes and more generally, when the curvature of flux tube becomes very large so that the inertia of the particle drives it to a larger space-time sheet. The model applies also to Z^0 magnetic case and if the particles are ordinary em ions, the generation of radiation is expected also now. Of course, also the collisions of neural particles generate also radiation but not so much.

This mechanism, besides providing a model for dissipation, might explain the luminous phenomena associated with tornadoes [35, 36, 37]. Tornadoes are expected to involve also ordinary magnetic fields and corresponding flux tube structures so that also they could give rise to luminous phenomena by the same mechanism as in the case of auroras.

e) In fact, the vortices of any hydrodynamic flow correspond to Z^0 magnetic vortices: in particular, the mechanism inducing transition from superfluidity to ordinary fluid flow is generation of Z^0 magnetic vortices at critical velocities which are much lower than those predicted by hydrodynamical arguments [D7]. The leakage mechanism of radial em or Z^0 supra currents from magnetic flux tubes might be involved with the dissipation and also with sono-luminescence.

4.1.2 Tornadoes as rotating magnetic and Z^0 magnetic systems

A useful analogy for the tornado is provided by rotating magnetic system known as Searl device [42]. This system starts to spontaneously accelerate at certain critical rotation frequency. The TGD inspired model for the system is discussed in [G2]. Spontaneous acceleration is accompanied by spontaneously occurring concentric cylindrical magnetic walls of thickness $\simeq .5$ cm with mutual distance of $\simeq .5$ m. Magnetic walls have thickness allowing the interpretation as scaled up counterparts of cell membrane for $k_d = 2$. Magnetic walls would contain dark matter Bose-Einstein condensates in cyclotron state carrying maximal magnetic field of $B = .05$ Tesla. Magnetic walls could serve as angular momentum and energy storages from which the system draws energy by time mirror mechanism which means sending of negative energy phase conjugate photons absorbed by the Bose-Einstein condensate.

The observed ionization of air in the vicinity of the rotating system is explained in terms of an Ohmic current generated by the radial vacuum electric field implied by the rotating magnetic field. Since the electric field corresponds to non-vanishing vacuum charge density, this current charges the rotating magnetic system. Current carriers drop from atomic space-time sheets to larger space-time sheets at the boundary of the system liberating their large zero point kinetic energy of order 1 keV. The resulting voltage allows in principle to use the system as an over-unity device by adding load to a wire connecting the system to ground. The model leads to the proposal that rotating magnetic flux quanta provide a fundamental mechanism leading to the generation of plasmoids, which can be regarded as primitive living systems [39].

The identification as a rotating magnetic system allows to interpret the luminous phenomena associated with tornadoes [35, 36, 37] in terms of a plasma resulting from the dropping of electrons of radial Ohmic currents to large space-time sheets. An analogous leakage to larger space-time sheets would be presumably associated with auroras. The angular momentum stored to dark Bose-Einstein condensates at the magnetic and Z^0 magnetic walls would provide angular momentum and energy for the tornado. As a matter fact, the formation of these Bose-Einstein condensates could force the rotation of tornado by angular momentum conservation.

4.1.3 Tornadoes as dark matter systems

The identification of tornadoes as large \hbar systems is suggested by the ability to self-organize and preserve the self-organization pattern for relatively long periods of time. Dark matter would imply self organization and make the system living in a primitive sense.

There are several kinds of tornadoes [38]. For supercell tornadoes called twisters the width is usually below $d = 90$ m but can sometimes extend over 1.6 km. Wind velocity is typically $v = 160$ km/h= 44 m/s. This gives rough estimate for the angular velocity associated with tornado as $\omega = v/d$. The corresponding frequency is $f = 1/2\pi$ Hz.

Assume that dark variants of $k = 113$ weak bosons are responsible for long range weak fields possibly involved with the rotating system and that also rotating magnetic fields defining something very much analogous to the inner magnetosphere of Earth are involved. Denote by k_d^{em} and $k_d^W = k_d^{em} + 2$ weak and em dark matter levels respectively and assume $\lambda = 2^{11}$.

a) For weak $k_d^W = 4 = k_d^{em} + 2$ the thickness of scaled up cell membrane like structure is $d_m = 2 + 2 = 4$ cm whereas $d = \lambda \times d_m = 80$ m corresponds to an upper limit for the size for super cell identified as a scaled up cell like structure in em case. $L_W = 2^{22} \times .2 \mu\text{m} = .8$ m defines the upper limit for the thickness of the weak magnetic walls. The appearance of d_m as upper bound for width of twister supports the similarity of the dynamics of twisters and rotating magnetic systems.

b) For weak $k_d = 5$ level one has $L_w = 1.6$ km, which suggests that largest tornadoes correspond to $k_d^W = 5 = k_d^{em} + 2$ systems. The prediction would be that magnetic walls of thickness 40+40 m are present at this level. Hurricanes having much larger width could correspond to $k_d^W = 6 = k_{em} + 2$ level of dark matter hierarchy with $L_W(5) = 3355$ km and $d_m(4) = 168 = 84 + 84$ km. This wall structure should reflect itself in the visible properties of tornadoes and hurricanes.

Consider now this picture more quantitatively in case of tornadoes.

a) Both em and Z^0 magnetic fields can be considered as being associated with the vortex and by previous argument would correspond to $k_d^{em} = 2$ and $k_d^W = 4$. A natural guess would be that magnetic flux quanta correspond to walls except in the central region where magnetic or Z^0 flux tube could exist as in the case of rotating magnetic systems.

b) In electromagnetic case only the cyclotron energies of electron Cooper pairs are stable and this only if the magnetic field at magnetic walls of thickness 4 cm is of the same maximal magnitude $B = 2^{10} B_E = .05$ Tesla as for rotating magnetic system. Cyclotron energy for electron is $E_c = 10$ eV

for $k_d = 2$. For proton Cooper pair E_c would be below 11 meV and below the thermal stability limit of .086 eV at room temperature.

c) Exotic neutrinos with $k = 127$ and having same mass scale as electrons are necessary if one wants to preserve the model for cognitive neutrino-antineutrino pairs [M6]. Note that these neutrinos do not contribute to the decay width of ordinary intermediate gauge bosons since they do not couple to them. The long range weak interaction mediated by dark $k = 113$ weak bosons essentially massless below the length scale L_W would make possible the formation of neutrino Cooper pairs by a mechanism similar to that applying in the case of electrons. Neutrino Cooper pairs could generate the Z^0 magnetic field inside Z^0 magnetic wall. The field would be given by $B_Z = 2K_Z$, where K_Z is the magnitude of oppositely directed neutrino Cooper pair surface currents at 2 cm thick boundaries of say .5 m thick Z^0 magnetic wall (this would conform with 2 cm+ 2 cm decomposition of boundary layer analogous to the decomposition of cell membrane to lipid layers).

Second possibility is provided by exotic O_2 and N_2 ions for which with atomic nuclei possess some charged color bonds making them both em and Z^0 ions. Exotic ions could form Bose-Einstein condensates in the Z^0 magnetic field created by surface supra currents of neutrino Cooper pairs. Weak length scale $L_w(k_d = 4) = .8$ m gives upper bound for the thickness of the Z^0 magnetic walls. This suggest that the distance $d = .5$ m between magnetic walls in Searl device could correspond to the thickness of Z^0 magnetic wall (parity breaking provides evidence for the presence of also Z^0 fields in the system).

For the thickness $d_W = .5$ m of Z^0 magnetic walls and for $g_Z B_Z = eB_E = .5$ Gauss $k_d = 4$ flux quantization condition is satisfied for the distances $R > 1$ m from the center of vortex. For neutrino Cooper pairs the order of magnitude for cyclotron energies is 44.6 keV and still considerably smaller than $k = 127$ neutrino mass. The order of magnitude for the exotic ion cyclotron energies is from flux quantization $E_c = (Z/A) \times E_p(k_d = 4) \simeq (Z/A) \times 21.8$ eV, where Z is the anomalous em charge of exotic ion and A its mass number. ($A = 24$ for O_2 and $A = 28$ for N_2) so that thermal stability is achieved at room temperature.

d) The rough estimate of the angular momentum, call it L , from the basic data and from the classical formula for cyclotron orbits, call it L_c , gives some grasp about the angular momentum storage idea. For Z^0 magnetic case the estimate for angular momentum using $L = MvR$ with $v = 40$ m/s, $R = 50$ m, and $M = Am_p$, is by a factor $(A/Z) \times (v/\omega_p R) \sim (A/Z) \times 2.7 \times 10^{-3}$ smaller that the classical estimate $L_c = M\omega R^2$, $\omega = ZeB/Am_p$, for $B = .5$

Gauss. For neutrino Cooper pairs L is 2.6×10^{-6} smaller than L_c . For electronic Cooper pairs L would be by a factor $\sim 1.3 \times 10^{-9}$ smaller than L_c so that quite impressive amount of angular momentum and also energy could be stored to cyclotron states (note however that for each value of principal quantum number n also state with $L_z = 0$ is possible).

4.2 Auroras as an astrophysical quantum phenomenon?

Auroras are perhaps the most magnificent electromagnetic phenomenon in the atmosphere. The mechanism generating the auroras is not completely understood. What is however known that auroras involve the motion of ions along flux lines of Earth's magnetic field acting effectively as current wires. This suggest the that the ionic currents could be supra currents running along the flux tubes of the magnetic field of Earth or its dark counterpart $B_{end} = 2B_E/5$ suggest to exist on basis of findings about the effects of ELF em fields on vertebrate brain [M3]. Hence auroras could be a directly visible macroscopic quantum phenomenon! In the following a model of auroras based on this vision and explaining the latest findings about them is developed.

4.2.1 Basic facts, ideas and puzzles related to auroras

Auroras occur at heights of 56-970 km along a circle surrounding the magnetic North (South) pole [29]. Magnetic storms accompany auroras and auroras are especially intense during sunspot maxima. Protons and electrons of the solar wind are known to flow along magnetic flux lines acting effectively as current wires. Some mechanism accelerates electrons and protons during their travel to the pole region where they collide with the ions (mainly oxygen and nitrogen) of the ionosphere and generate visible light. The spectral lines correspond to ionic transitions and each color corresponds to a particular ion dominating at a particular height.

A brief summary of the basic ideas and problems related to the auroras is in order before representing TGD based model.

a) The reconnection of solar magnetic field lines carried by solar wind with the field lines of Earth's magnetic field was proposed by James Dungey as a mechanism explaining the energetics of the auroras. There is indeed increasing empirical support for the view that the reconnection of the magnetic field lines of Sun and Earth accompanies auroras [34, 31, 32]. What would happen would be that the reconnected nearby opposite fields lines form a tightly bent U-shaped structure which straightens and acts as a cat-

apult giving recoil energy to the plasma ions flinging in the direction of Earth. The highly energetic protons and electrons of the solar wind would flow towards Earth and collide with the ions of atmosphere and generate the auroras in this manner. The detailed understanding of the reconnection mechanism is lacking and here TGD suggests microscopic topological description relying on magnetic flux tubes.

b) The problem of the reconnection mechanism is how the solar and earthly magnetic flux lines running in opposite directions and carrying opposite currents know of each other and can change their direction so that the lines can meet. In TGD framework the reconnection of the magnetic flux tubes could be seen as a process changing space-time topology. At the point of reconnection magnetic field becomes zero in Maxwell's theory and it is thought that the charged particles must be able to leave the flux lines by some unknown mechanism so that demagnetization occurs. TGD in turn suggests that inertial effects force ions flow to larger space-time sheets along join along boundaries bonds.

c) An electric field parallel to the magnetic flux lines has been postulated as the mechanism of acceleration: empirical evidence for the existence of this electric field has been found quite recently [33]. Two U shaped potential regions with positive *resp.* negative charges have been found at heights 5000-8000 km *resp.* 1500-3000 km. It is convenient to christen lower U shaped region as \cap and the upper one as \cup . The negatively charged region feeds electrons to the aurora region and positively charged region sucks them back. There is however no consensus about how this kind of electric field is generated and how it could be stable.

4.2.2 TGD based model for auroras

There are several poorly understood aspects related to the modelling of auroras. TGD approach provides new views to these problems. The following vision is perhaps the most plausible option discovered hitherto.

a) The electronic and protonic currents in the ionosphere of Earth would flow as supra currents for $k_d = 4$ level of dark matter hierarchy. If the flux tubes of solar wind and of magnetotail have $k_d = 5$, the flux tubes inside and outside ionosphere would be roughly of the same transversal area. For this option electron Cooper pairs and bosonic ions up to atomic number $A \leq 16Z$ can form Bose-Einstein condensates $k_d = 5$ flux tubes.

b) The reconnection of field lines generalizes to reconnection of magnetic flux tubes. The large inertia of ions in reconnection process from solar wind flux tube can induce their leakage and subsequent transfer to the upper

magnetic flux tube in reconnection process. This would accumulate negative charge to the lower and positive charge to the upper U shaped flux tube.

c) The rapid straightening of the lower U shaped flux tube behaving like rubber band provides the mechanism of acceleration and brings ions of solar wind to the ionosphere where the collision with the flux tubes of inner magnetosphere induces the collision of electrons and ions and generates auroras. The liberation of cyclotron energy of electrons in cyclotron transitions of Bose-Einstein condensate of Cooper pairs of electrons and protons, and possibly even of exotic O^+ ions makes possible ionization and electronic excitations of ions involved.

1. Could em currents flow along magnetic flux quanta of solar and Earth's magnetic field as supra currents?

The question is under what conditions the statement that charged particles move along the flux lines of Earth's magnetic field without appreciable dissipation translates in TGD framework to supra currents flowing along the flux tubes of Earth's magnetic field.

a) Consider first the flux tubes of solar wind. The solar wind is made of Hydrogen (95%) and Helium (4%) and Carbon, Nitrogen, Oxygen, Neon, Magnesium, Silicon and Iron ($\simeq 1\%$). The magnetic field has strength ~ 10 nT. Electron Cooper pairs at $k_d = 4$ level of dark matter hierarchy would have cyclotron energy $E_c = 8$ eV which is below the temperature $T \simeq 15$ eV of solar wind near Earth but proton Cooper pions and ion Coopers would not satisfy it. For $k_d = 5$ $E_c(e) = 16$ keV implies that electronic Cooper pairs satisfy the stability condition. Protonic cyclotron energy would be 8 eV and below the thermal stability limit.

b) Consider next flux tubes in magnetotail. In magnetotail the field strength of Earth's magnetic field is around 30 nT in the lobes of the inner magnetosphere at the night side of Earth and temperature is around .5 eV (metabolic energy quantum again) so that critical cyclotron energy is $E_{cr} = 2.88 \times T = 1.44$ eV. Proton's cyclotron energy would be 12 meV for $k_d = 4$ so that Cooper pairs would not be possible in magnetotail. For electron the cyclotron energy would be 24 eV. An interesting question is whether Bose-Einstein condensates of exotic O^+ ions could be present near polar regions where field is stronger. What is known that cyclotron resonance frequencies of O^+ and H^+ ions appear in the frequency spectrum of electric fields in the aurora regions [40]. This however requires only $k_d = 4$ since magnetic field is much stronger and near to $B_E = .5$ Gauss.

For $k_d = 5$ the value of electron cyclotron energy in magnetotail would be 48 keV and 10 percent of electron rest mass. Also ions with mass number

$A \leq 16Z$ would have cyclotron energies above the thermal threshold. What is interesting and perhaps of significance is that O^+ exotic ion would be the heaviest possible ion forming Bose-Einstein condensates and also the dominating one besides proton.

The transversal areas of magnetic flux quanta inside ionosphere ($B_{iono} \sim .5$ Gauss) and in magnetotail $B_{tail} \sim 30$ nT are very nearly the same if ionosphere corresponds to $k_d = 4$ and magnetotail to $k_d = 5$ (the ratio of the nominal values is $B_{iono}/B_{tail} = 1667 \sim \lambda$).

2. Radii of flux quanta

The gyroradius p_T/ZeB , where p_T is momentum transversal to B , of proton *resp.* electron of solar wind in the magnetotail is about 700 km *resp.* 20 km whereas the radii of the magnetic flux tubes would be in the range in 10-100 micrometers for ordinary value of \hbar and minimal magnetic flux.

For $k_d = 5$ level of dark matter hierarchy the radius of tubular flux tube scaling as $\hbar^{1/2}$ is $R_n = \sqrt{n} \times R_1$, where $R_1(B_{wind} = 10 \text{ nT}) = 6$ km and $R_n(B_{tail} = 30 \text{ nT}) = 10$ km. If the radius is required to be above the electronic gyroradius for both wind and magnetotail, one must have $n \geq 11$ for B_{wind} and $n \geq 4$ for B_{tail} . Flux tube radii are very nearly identical for minimal values of n . These observations favor $k_d = 5$ option.

That the gyroradii of ions are larger than the radius of the flux tube for $k_d = 5$ implies that the ions leak out from solar flux tube in the reconnection process. This turns out to be essential for how the negatively and positively charged regions are generated in the reconnection process.

3. Reconnection mechanism

In TGD framework one can understand how reconnection can occur. The helical structure of the flux tubes implies that they can be in transversal direction to the average magnetic field and this means that flux tubes can meet each other in U-shaped manner. Thus the process of reconnection would be a genuine quantal and topological transition for which the flux quantization would be essential.

It seems natural to expect that the location of the reconnection region is determined from the requirement that the flux tubes of solar wind and Earth's magnetic field have same thickness so that also local magnetic fields have the same strength from flux quantization. In Maxwell's theory this corresponds to the fact that the two magnetic fields sum up to zero. The reconnection process should be also energetically favored.

4. Acceleration mechanism

One can regard Earth's magnetic field as a collection of magnetic flux tubes containing matter and analogous to rubber strings. For instance, the rotation of the magnetic flux tubes could be essential prerequisite for the stability of curved flux tubes. Also the idea about catapult action meaning that the reconnected U shaped magnetic flux tube in East-West plane, briefly \cap , rapidly straightens and becomes a flux tube in ionosphere and collides with flux tubes of ionosphere looks natural. $k_d = 5 \rightarrow k_d = 4$ phase transition would naturally accompany this process.

The collision of flux tubes would in turn induce the collision of ions and electrons inside them and generate auroras. For $k_d = 5$ the high energy scale $E_c = 48$ keV of the cyclotron energy states of electrons would induce ionization of atoms in the magnetic flux tubes and induce generation of visible light in atomic transitions of ions and also generation of X rays and perhaps even gamma rays. Even when the phase transition to $k_d = 4$ state occurs inside ionosphere, the cyclotron energy scale is 24 eV and cyclotron photons are in UV region. Analogous collision of flux tubes could explain generation of X and gamma rays associated with lightnings.

5. Formation of return current and generation of strong voltage between reconnection region and aurora region

This picture allows also to understand why a return current from aurora region to \cup is formed and what might cause the strong voltage of about 10^4 Volts between the top of \cap and ionosphere.

The formation of the return current of electrons suggests the presence of closed electric field lines so that electric field would not be conservative. These closed field lines would correspond to closed structures formed from magnetic flux tubes carrying electric field. This means that there must be time varying magnetic flux through the surface, call it X^2 , orthogonal to Earth's surface and extending from the aurora region in ionosphere to \cup . This is the case if the highly curve \cap contracts (recall the rubber band analogy) to a relatively straight flux tube inside ionosphere in magnetic East-West direction. The change of the magnetic flux through X^2 would be the magnetic flux carried by this flux tube. Of course, several flux tubes might be involved.

The generalization of the flux quantization condition to time domain reads as

$$2e \int_0^T V dT = n\hbar(k_d) ,$$

where T is the time during which flux tube traverses the boundary of iono-

sphere. The condition follows from Faraday's induction law and magnetic flux quantization, and relates the change of flux to the time and nonconservative voltage around flux loop. If n refers to the flux of single flux tube of Earth's magnetic field in which case it would have radius $R_n = \sqrt{n} \times 10$ km, $n \geq 4$ by the requirement that electron gyroradius is smaller than R_n . Alternatively, one could have m flux tubes with minimal radius $R_{tail} = 20$ km corresponding to $n_{min} = 4$ flux quanta giving $n = 4m$.

This condition allows to estimate the value of T using the estimate $V = 10^4$ V [41] for the voltage between recombination region and auroral region. For $n = 4m$ for B_{tail} $k_d = 5$ gives $T = m \times 97$ s for the time during which the flux tube traverses the boundary of the ionosphere. In [33] 200 s time scale is associated with the straightening process on basis of experimental data. This would support the idea about quantal process and $m = 2$ is favored if the estimate is taken completely seriously. This would mean radius 28 km safely above the electronic gyroradius 20 km. For $k_d = 5$ the radius of the flux tube would be $R = \sqrt{m}R_0$, $R_0 = 20$ km so that the velocity of straightening flux tube would be $v \sim 2\sqrt{m}R_0/T = .4\sqrt{m}$ km/s.

7. Generation of regions of positive and negative charge

The proposed reconnection mechanism provides also insights to the mechanism leading to the generation of negative charge to the top of \cap at height 1500-3000 km above Earth and positive charge to the bottom of \cup at 5000 – 8000 km above Earth [33]. The formation of these regions can be indeed understood: due to the small inertia of electron Cooper pairs of solar wind and the fact that the electronic gyroradius 20 km is smaller than the radius of flux tube of Earth's magnetic field in magnetotail for $k_d = 5$, electrons are not expected to leak out of the flux tube in the reconnection process. Ions are however much more massive and their gyroradius (700 km for proton) is much larger than 20 km so that they are expected to leak out in the reconnection process and end up to \cap thus providing it with a positive charge.

4.2.3 Auroras, meteors, and consciousness?

There are claims that auroras generate audible sounds [29]. These sounds have not been detected by acoustic means. Magnetic sensory canvas hypothesis could explain this. The magnetic storms accompanying auroras should affect also our auditory canvases. In particular, Schumann resonances which could correspond either MEs parallel to the magnetic flux tubes or oscillations of the magnetic flux tubes, are excited. Higher Schumann resonances

are in the audible range and could directly give rise to extrasensory perception of sounds. The TGD based model of hearing relies heavily on classical Z^0 fields and auditory canvas could be actually Z^0 magnetic. Since all classical fields are expressible in terms of CP_2 coordinates, magnetic storms are expected to be accompanied by their Z^0 magnetic counterparts.

There is also some other evidence for the sensory canvas hypothesis. Since 16th century it is known that also meteors produce audible sounds. What is mysterious that there is no time lag due to the propagation through the atmosphere. The explanation is that it is very low frequency em waves which propagate to Earth and generate sounds by interacting with the objects at the surface of Earth. Joined by the International Leonid Watch - Croatia (ILWC) project, a group of scientists presented the first instrumental detection of elusive electrophonic meteor sounds. In November 1998, the researchers from the Croatian Physical Society and the University of Kentucky organized an expedition to Mongolia to observe the anticipated Leonid meteor shower and shed some light on the phenomenon [30]. The complete data analysis revealed two electrophonic (electronically detected) sounds that provided several important clues about the nature of this long-standing astronomical mystery. It became clear that sounds were created when the meteors were crossing night-time ionosphere. The existing theories cannot however completely explain the phenomenon. The energy of meteor does not seem to be high enough to invoke the electric fields needed to explain the electronically recorded sounds, and strangely enough, the frequencies are much lower than expected, in the region 20-40 Hz.

Magnetic mirrors as carriers of the electromagnetic perturbations might allow a better understanding of the phenomenon. Perhaps the audible sounds, in contrast to the electronically recorded ones which seem to be of much lower frequency, are in fact generated by the direct perturbations of magnetic or Z^0 magnetic auditory canvas: this would explain why there is no lag due to the propagation through atmosphere. Electronically recorded sounds could be induced by the em perturbations propagating along magnetic mirrors at Schumann frequencies and the mirrors might act as resonators amplifying the em fields (electrophonic sounds had frequency spectrum in the region of lowest Schumann frequencies). Notice that magnetic mirrors of length shorter than Earth's circumference would give rise to higher resonance frequencies than Schumann frequencies.

There are also reports that seeing auroras can cause a loss of consciousness. This effect might not be only due to the depth of the aesthetic experience. The effects of magnetic storms on patients of mental hospitals are also well documented. If our sensory representations are indeed realized at

magnetic flux tubes structures associated with Earth's magnetic field, one is led to ask whether the dissipative processes associated with auroras destroying ionic supra currents might indeed affect directly our consciousness, inducing even a loss of consciousness.

The magnetic flux tube structures associated with the sensory canvas could also experience the pressure of the solar wind and change their shape during night time. Also this might correlate with the fact that we usually sleep during night time and daytime consciousness differs from nighttime consciousness.

4.3 Lightnings, sprites, elves, and the hypothesis of magnetic sensory canvas

In 1920s, the Scottish physicist C. T. R. Wilson predicted the existence of brief flashes of light high above large thunderstorms [45]. Almost 70 years later, Bernard Vonnegut of SUNY Albany realized that this prediction could be tested by studying the videos of Earth's upper atmosphere recorded by space shuttle astronauts. William Boeck and Otha Vaughan from NASA decided to look for the evidence and they indeed found it. Also John Winkler and his colleagues had serendipitously observed a flash in moonless night time skies over Minnesota in 1989. These findings inspired two field programs (led by Walter Lyons and Davis Sentman respectively) to study the new phenomena and it soon became clear that the flashes are in fact a common phenomenon in the mesosphere.

Sentman and Lyons found two broad classes of flashes [43, 44]: sprites and elves. These short lived luminous phenomena are associated with large thunder storms called mesoscale convective systems often covering entire states in the Great Plains of the US in summertime. These migratory regions contain often regions of active convection adjacent to the regions of weaker stratiform convection. Ground flashes with a negative polarity (Earth surface corresponds to the negative electrode) dominate in the active convection regions whereas the less frequent but more energetic flashes with positive polarity (Earth surface corresponds to positive electrode) predominate in the stratiform regions. The great majority of sprites and elves are initiated by ground flashes of the latter type. Elves and very low frequency perturbations from electromagnetically pulsed sources are centered above vertical channels to ground whereas sprites lie above horizontally extensive spider lightnings in the lower portion of the stratiform cloud.

My own interest on these phenomena was stimulated by the article [46] according to which neither the origin of the blue light accompanying sprites

nor the fast rate for the development of sprites are well-understood. The obvious strategy is to find whether the notion of many-sheeted space-time could provide an improved understanding of these phenomena.

The notion of many-sheeted space-time is crucial for TGD based model of brain involving in an essential manner also the notion of the magnetic sensory canvas: the magnetic flux tube structures involved can have size comparable to Earth's size. An interesting question is whether one could somehow relate the notion of sensory magnetic canvas to the electromagnetic phenomena occurring in the atmosphere. Rather encouragingly, the basic dynamical time scales of lightnings, sprites and elves correspond to those associated with brain. This inspires some speculations about how magnetic bodies and atmospheric electromagnetic phenomena might relate.

4.3.1 Lightnings

A good summary about basic facts concerning lightnings [47], sprites and elves can be found in Wikipedia [48]. Lightnings are classified to positive and negative lightnings depending on whether the electron current is from ground to cloud or vice versa. The following brief summary gives a rough account of what happens in case of negative lightning for which electron current flows to ground.

An initial discharge, (or path of ionised air), called a "stepped leader", starts from the cloud and proceeds generally downward in a number of quick jumps, typical length 50 meters, but taking a relatively long time (200 milliseconds) to reach the ground. This initial phase involves a small current and is almost invisible compared to the later effects. When the downward leader is quite close, a small discharge comes up from a grounded (usually tall) object because of the intensified electric field.

Once the ground discharge meets the stepped leader, the circuit is closed, and the main stroke follows with much higher current. The main stroke travels at about $0.1 c$ and has high current for .1 m or so. It may persist for longer periods with lower current.

In addition, lightning often contains a number of restrikes, separated by a much larger amount of time, 30 milliseconds being a typical value. This rapid restrike effect was probably known in antiquity, and the "strobe light" effect is often quite noticeable.

Positive lightning does not generally fit the above pattern.

Positive lightnings are rare but more energetic. The typical voltages, electric fields, and durations of strikes involved with positive *resp.* negative lightnings are 1 GV, 10^5 V/m and 1 ms *resp.* .1 GV, 10^4 V/m and .1 ms.

During positive lightning there is a huge amount of VLF and ELF radiations which implies that lightning induces effects in ionospheric scale.

The notions of leader emerging from cloud and streamer emerging from ground and meeting before the strike are well established. The development of leader means that air becomes conductive in a stepwise manner by ionization. Stepped leaders are associated with negative lightnings and dart leaders with positive lightnings. Lightnings are accompanied by X ray bursts with duration $< .1$ ms. with X ray energies up to few hundred keV. The bursts are presumably generated during stepped leader and dart leader phase. Also gamma ray bursts have been observed.

Runaway breakdown is a generally accepted mechanism in the theory for the formation of lightnings. It is assumed that cosmic ray strikes atmospheric molecular and releases extremely energetic electrons having enhanced free path length of tens of centimeters. Electrons are accelerated in the electric field of storm and ionize further molecules and initiate the runaway breakdown at higher which then proceeds downwards. Conductive path with a length of typically 50 m is created. There are however some problems. The rate for the strikes by cosmic rays having sufficient energy is $50/\text{km}^2$ and too low to explain the number of lightnings during thunderstorm. Also the measured X ray burst intensity is only 5 per cent of the predicted value.

4.3.2 Sprites

Sprites come in several varieties and these complex structures have been dubbed with descriptive names like carrots, angles, jellyfish and A-bombs. The simplest sprites are so called C sprites which have transversal size of order 200 m and height of order 10 km and form structures resembling Fourth of July fireworks. The vertical extension of sprites can be as high as 60 km and their lower end is typically at the height of 30 km (for illustrations of sprites and elves see [46]).

In Wikipedia [47] sprites are characterized as follows.

Sprites are now well-documented electrical discharges that occur high above the cumulonimbus cloud of an active thunderstorm. They appear as luminous reddish-orange, neon-like flashes, last longer than normal lower stratospheric discharges (typically around 17 milliseconds), and are usually spawned by discharges of positive lightning between the cloud and the ground.

Sprites can occur up to 50 km from the location of the lightning strike, and with a time delay of up to 100 milliseconds. Sprites usually occur in clusters of two or more simultaneous vertical discharges, typically extending

from 65 to 75 km above the earth, with or without less intense filaments reaching above and below. Sprites are preceded by a sprite halo that forms because of heating and ionisation less than 1 millisecond before the sprite.

The structure of sprite resembles that of a botanic tree consisting of roots (negative end), trunk and branches (positive end). This bi-directional structure of the sprite suggests two separate processes: the first process proceeds upwards and is followed by a second process proceeding downwards. The blue color of the lower part of the sprite (roots) is known to be due to the transitions of N_2^+ ions whereas the red color of the upper part is due to the transitions of N_2 molecules.

Wilson's theory suggests that the process associated with trunk and branches of the tree corresponds to a dielectric breakdown induced by the ionization of molecules by electrons flowing upwards in the electric field generated by the spider lightning. The dipole field associated with the lightning behaves as $1/z^3$ as function of height from the pancake like electronic reservoir located at the thunder cloud at height of order 10 km. Since the dielectric strength (the critical electric field causing the ionization of molecules) is proportional to the density of the molecules, which decreases exponentially with height, the dielectric breakdown is predicted to begin from higher heights above thunder cloud and cause a cascade like electron current.

The expression for the drift velocity of electron in an external electric field is obtained from the condition

$$\frac{m_e v^2}{2} = eEl \quad , \quad l = \frac{1}{n\sigma} \quad . \quad (16)$$

Here σ denotes the total scattering cross section for the scattering of electrons on molecules and l denotes the length of the average free path of electron. The condition simply states that the kinetic energy gained in the field between two interactions equals to the work done by the electric field on electron.

Ionization becomes possible when the kinetic energy is above the ionization energy E_{ion} of the molecules of the atmosphere. This condition determines the critical value of the electric field as

$$eE_{cr} = 2E_{ion}n\sigma \quad . \quad (17)$$

The critical value of the electric field is proportional to the density n of the molecules decreasing exponentially with height. The values of the dipole

moment p characterizing the electric fields generated by lightnings range from 10 to more than 10^3 coulomb kilometers (for the convenience of the reader we notice that one coulomb corresponds roughly to 10^{19} electronic charges). Assuming the distance scale $z \sim 40$ km, dipole moment $p \sim 10^3$ Ckm, and collision cross section $\sigma \sim \text{Angstrom}^2$, one finds that the critical drift velocity is of the same order of magnitude as the observed velocity .1 c for the generation of sprite. In [46] it has been stated that the predicted critical drift velocity tends to be too small.

The negative end of the sprite (roots) accompanied by blue light suggests that the N_2^+ ions created in the electronic ionization run downwards in this region. The mechanism leading to the the transitions of N_2^+ ions generating blue light is most naturally the collisions of N_2^+ ions with N_2 molecules. This assumption conforms with the basic facts about sprite formation and structure: the intensity of the blue light is comparable to that of red light, the blue end of the sprite develops later than the red end, the blue emission is at the lower end of the sprite, and the branching of the lower end proceeds downwards. Note that the critical velocity for the ionization of N_2 molecules by collisions with N_2^+ molecules is proportional to $1/\sqrt{M(N_2)n}$ and thus considerably smaller than in case of electron for given values of n and E . This together with the larger density of N_2 molecules implies that the lower part of the sprite is generated more slowly.

A priori also sprites for which thunder cloud carries positive charge are possible. Only two cases of sprites associated of this kind have been found, and according to [46] this asymmetry is not yet well-understood. A possible explanation is following. When cloud is negatively charged, the pancake like electronic reservoir located at the thunderstorm provides the seed electrons initiating the ionization cascade providing new current carrying electrons. When the cloud is positively charged, the electrons would propagate downwards from upper part of atmosphere to the direction in which drift velocity decreases. There are however no seed electrons now. There is however a reservoir of positive N_2^+ ions in thunder cloud and they might be able to generate the dielectric breakdown. It is quite possible that the typical seed density is simply too low for this in most cases. These infrequent sprites should have blue or pink-blue upper end ($N_2^+ - N_2$ collisions can also excite N_2 molecules) and should develop with much more slower rate.

If the collisions with the electrons were responsible for the transitions of N_2^+ ions (as believed in [46]), the intensity of the blue light would be by several orders of magnitude weaker from the fact that the density of N_2^+ ions is of the same order as that of electrons from the requirement of overall charge neutrality, and from the fact that the density of N_2 ions is much

higher than that of electrons (there are roughly 1 electron per 10 billion N_2 molecules [46] at the upper portion of the sprite).

4.3.3 Elves

In Wikipedia [47] elves are characterize in the following manner.

Elves often appear as a dim, flattened, expanding glow around 400 km (250 miles) in diameter that lasts for, typically, just one millisecond [7]. They occur in the ionosphere 100 km (60 miles) above the ground over thunderstorms. Their colour was a puzzle for some time, but is now believed to be a red hue. Elves were first recorded on another shuttle mission, this time recorded off French Guiana on October 7, 1990. Elves is a frivolous acronym for Emissions of Light and Very Low Frequency Perturbations From Electromagnetic Pulse Sources. This refers to the process by which the light is generated; the excitation of nitrogen molecules due to electron collisions (the electrons having been energized by the electromagnetic pulse caused by a positive lightning bolt).

Elves are thus a phenomenon occurring above ionosphere rather whereas sprites are ionospheric phenomena. This allows to understand why they occur for positive lightings (electrons flow from ground to cloud).

In case of elves the ionization mechanism differs from that for sprites. The radiation from the lightning decays with distance as $1/z$ and this guarantees that the threshold for the breakdown is exceeded as long as lightning current is sufficiently large. The observations show that there is a time lapse of order 10 ms between the lightning and the generation of elve: this lapse is consistent with the propagation of radiation with light velocity. Observations show that peak currents of 70 A or greater are required.

Electronic plasma frequency defined as

$$f_p^2 = \frac{n_e e^2}{m_e} \quad (18)$$

plays an important role in understanding the electromagnetic phenomena in atmosphere. Plasma frequency defines the cutoff frequency for waves which can propagate inside sprite: what this means is that frequencies lower than f_p are reflected. The observations about reflections of em waves on sprites show that f_p is in the range 2 – 25 kHz which means that the density of electrons is in the range 10^4 to 10^6 cm^{-3} , somewhat more dilute than in aurora borealis and slightly above the electron concentration in the daytime E region of the ionosphere. VF and ELF em waves can propagate in the

80-90 km thick wave guide below ionosphere and sprite activity generates ELF waves, which are especially strong at Schumann resonance frequencies and serve as a global signature for them.

4.3.4 Dark matter hierarchy, lightnings, sprites, and elves

What is known about sprites and elves might be marginally understood in the framework of standard physics. The model for the leaders based on runaway breakdown induced by cosmic rays is however inconsistent with all empirical facts and $k_d = 4$ Bose-Einstein condensates at the flux tubes of Earth's magnetic field provide an alternative model. This inspires the question whether dark matter hierarchy could manifest itself somehow in these phenomena. The first thing one can do is to look whether the time and length scales involved could be assigned with the basic scales of the dark matter hierarchy.

1. Time scales

Millisecond time scale seems to govern the dynamics of both lightnings, sprites and elves. The net time for the formation of stepped leader is about 200 ms and since length scale involved is 10 km this means that generation of single step corresponds to millisecond time scale. Also the time scales of strikes are in millisecond scale: for instance, sprite halos appear 1 millisecond before sprite, sprite typically last about 17 milliseconds, and elves last for 1 millisecond.

The appearance of millisecond time scale for the main strike and appearance of re-strikes brings strongly in mind nerve pulse generation and nerve pulse sequences having similar time scales. Moreover, delta band of EEG resembles corresponding region of spherics and intense VLF and ELF radiation accompanies positive lightnings. The question is whether the similarity of time scales is a mere accident and whether lightnings could be regarded as sequences of scaled up nerve pulse like discharges involving kHz synchrony.

Taking this idea seriously, one can ask whether one could understand the emergence of 1 kHz frequency as a drum beat analogous to say 1 Hz cyclotron frequencies assignable to DNA in living matter and near to the thermal threshold for $k_d = 4$ cyclotron energies. Tornadoes involve luminous phenomena and thunderstorms. The model of tornadoes involves magnetic walls with Earth's magnetic field strength scaled up to .05 Tesla and naturally resulting from $Z = 2$ flux quantization with flux quantum area scaled down as $1/\lambda^2$ in the transition $k_d = 4 \rightarrow 3$. This transition would scale up 1 Hz delta frequency to 1 kHz frequency. Hence kHz band of spherics

could indeed play the role of drum beat in the generation of lightnings as atmospheric "nerve pulses".

2. Length scales

a) The length scales for the formation of leader seem to correspond to $k_d = 2$. Enhanced electron mean free path of few centimeters would correspond to a scaled up cell membrane thickness $4=2+2$ cm and the length 50 m of single step in leader to the scaled up maximal size scale of cell 80 m at this level.

b) The distances between sprites and lightning system are below 50 km. The maximal size of $k_d = 3$ variant of scaled up cell nucleus ($L(169)$) is about 40 km. Hence sprites could make thunderstorm a $k_d = 3$ phenomenon whereas elves would extend it to $k_d = 4$ phenomenon.

c) The generation of lightning could proceed from $k_d = 2$ level to higher levels of dark matter hierarchy. This kind of hierarchical development could explain the sprites and elves as well as strong ELF and VLF is associated with positive lightnings as being to the fact that electron current proceeds upwards and can thus excite $k_d = 3$ ionospheric excitations (sprites) and $k_d = 4$ excitations (elves) above ionosphere.

3. Dark matter hierarchy and generation of leaders

Dark matter hierarchy suggests a new kind of mechanism initiating the development of leaders. The dissipation-free acceleration of cyclotron electron Cooper pairs and of ions at the flux tubes in strong electric field and transfer to the atomic space-time sheets could provide a mechanism generating the typically 50 meter long steps of step leaders. The energy of .5 MeV, which corresponds to electron rest mass, would be reached in a free acceleration of proton or electron Cooper pair in an electric field of $E = 10^4$ V/m associated with negative lightnings over distance 50 meters. This corresponds to electron rest mass so that also the generation of gamma rays could be understood. For dart leaders the same energy would be reached during 5 meter long free acceleration, which raises the question whether dart leaders are step leaders with shorter length of the basic step.

Note that 80 m length scales corresponds to the maximal size of the fractally scaled up cell structure for $k_d = 2$ and that $k_d = 2$ dark matter level was already associated with tornadoes often accompanied by thunder storms.

Electronic cyclotron energy scale for $k_d = 4$ level of dark matter hierarchy is about $E_c = 33$ keV. Therefore cyclotron photons emitted in the collisions of electron Cooper pairs at the magnetic flux tubes of Earth could

be involved with the generation of highly energetic electrons which in turn induce runaway breakdown. This energy is perhaps too small to explain the energies of highest X rays and of gamma rays.

4. $k_d = 4$ dark matter and the formation of sprites and elves

The too low drift velocity of electrons drifting to the trunk and branches of sprite from electron reservoir at the bottom of the cloud is a possible problem in the model for the formation of sprites. Almost dissipation free upwards directed acceleration of Cooper pairs of electrons at $k_d = 4$ magnetic flux tubes would allow much higher drift velocities since the free path of electron Cooper pair would be longer. This would reduce the critical value of the electric field and make the process faster.

The density of N_2 molecules is about $10^3/\mu m^3$ at the upper part of the sprite and one can consider the possibility that at least part of these molecules reside at the magnetic flux tubes of the dark counterpart B_{end} of the Earth's magnetic field B_E which is hypothesized to have the value $B_{end} = 2B_E/5$ on basis of the model explaining the effects of ELF em fields on vertebrate brain (see the appendix of [J2] and [M3]). One can even raise the question whether singly charged exotic N_2^+ ions (behaving like neutral atoms electronically) could be present and define cyclotron condensates. The downwards directed dissipation-free acceleration of N_2^+ exotic ions scattering from ordinary N_2^+ ions could induce the transitions of N_2^+ ions responsible for the blue color in the lower part of sprite.

In the case of elves the ionization mechanism is believed to involve radiation from lightning energizing electrons in turn exciting N_2 molecules. The effect would be stronger if Bose-Einstein condensate of exotic N_2^+ ions is excited coherently by the collisions with energized electronic Cooper pairs.

4.3.5 Atmospheric electromagnetic phenomena and consciousness

The hypothesis about magnetic sensory canvas should be related to experimental reality somehow. The electromagnetic phenomena (such as lightnings, auroras sprites, elves) in the atmospheric waveguide are indeed rather promising in this respect.

a) If the magnetic sensory canvas hypothesis holds true one has the right to expect that brain functioning and these electromagnetic phenomena should possess common time scales. Amazingly, the frequency spectra as well as typical durations for the lightnings, sprites and elves correspond to those associated with brain. The typical duration of lightning is about .1

seconds which is the fundamental time scale of sensory consciousness and defines the duration of the memetic code word. Sprites are generated during one millisecond and typically last 10-100 milliseconds. The spectrum of the spherics associated with the activity of lightnings is in the range 0-25 kHz: this follows from the fact that waves in this frequency range are reflected from ionosphere and propagate in the waveguide defined by the atmosphere. It is perhaps not an accident that this frequency range corresponds to the range of frequencies audible for human brain.

It is also known that hippocampus, which is crucial for long term memories, contains highly ordered magnetite particles (private communication) and responds in complex ways to magnetic perturbations having frequencies in ELF range and amplitudes in picoTesla range. Perhaps it is not an accident that the amplitudes for the perturbations of Earth's magnetic field are also in picoTesla range in theta and alpha range of EEG frequencies. Also alpha waves generate a peak in MEG with amplitude of order picoTesla: presumably this peak corresponds to the lowest Schumann frequency. Also eyes generate static magnetic fields with strength of order 10 picoTesla. In consistency with the observations of Blackmann and others about the intensity and frequency windows for ELF em fields, these findings encourage to think that brain is indeed sensitive to the perturbations of Earth's magnetic field (note however that the electric fields in these experiments are typically of order 1 – 10 V/m [21] and roughly two orders of magnitude higher). This would mean also a sensitivity to the perturbations of the magnetic flux tube structures defining the hierarchy of magnetic bodies. These perturbation might directly affect conscious experience (not necessarily at our level of hierarchy) giving rise to effective extrasensory perceptions and the effects at the level of brain would represent a reaction to this kind of conscious experience.

b) There should be also interaction between brain and the electromagnetic phenomena in the atmosphere and Schumann resonances which characterize the perturbations of Earth's magnetic field should be of special importance. Lightnings, sprites and elves indeed excite Schumann resonances known to affect strongly human consciousness [23]. Furthermore, the shape of the frequency spectrum for spherics at delta frequencies resembles delta band of EEG [1]. The generation of Schumann resonances might mean also a direct interaction with the magnetic sensory canvas and one cannot exclude the possibility that atmospheric phenomena could have role in signalling at the higher levels of self hierarchy. Perhaps the peak in MEG at alpha range results from this kind of interaction.

There are typically few sprites per minute and they generate strong Schu-

mann resonances. One can wonder whether sprites and/or the associated spider lightnings could have correlates at the level of EEG and neurophysiology and perhaps even affect conscious experience, say by causing changes in mood. It should be possible to check whether the EEGs of persons possibly located at different parts of globe display simultaneous correlates for sprites and lightnings.

c) One could go even further and try to test the fractality hypothesis. The ratio of length scales associated with pairs cell membrane-cell, cortex-brain and atmospheric waveguide-Earth are of same order of magnitude. This observation and Mother Gaia hypothesis encourages to consider the possibility that the atmosphere could in some sense be a scaled-up version of cortex, which in turn would be scaled-up version of the cell membrane. For instance, the transversal size of order 200 m of the smallest sprites (so called C sprites) would correspond to the micron length scale in brain length scale and thus the size of smallest neurons whereas this length scale corresponds to nanometer (DNA size scale) at neuronal level. The height of C sprites which is about 10 km corresponds to the length of about 50 microns which in turn reminds of the lengths of cortical neurons.

d) The geometric appearance of sprites brings in mind the geometry of neurons and one can even play with the thought that sprites and lightnings are associated with pre-existing electric flux tube structures in atmosphere so that lightnings, sprites and elves could be phenomena comparable to nerve pulse activity and graded potentials in brain. The geometric structures associated with sprites resembles the axonal and dendritic geometries for cortical neurons.

e) The most fascinating possibility is that sprites and elves are parts of magnetic bodies made temporarily visible. If so, then one could also consider the possibility that magnetic bodies form a self hierarchy analogous to that formed by monocellulars and increasingly complex multicellulars with cell being replaced with brain/physical body of organism. Various organisms would obviously form the lowest level of this self hierarchy and various levels of collective consciousness would be the electromagnetic analog of the multicellular life.

4.3.6 What auroras, tornadoes, ball lightnings, and cold fusion might have in common?

If the density of the ions inside magnetic flux tubes is constant, garden hose instability for magnetic field suggests itself strongly. Similar instability might be associated with the flux quanta of the Z^0 magnetic field if they

contain Z^0 ions. This kind of instability of Z^0 magnetic field giving rise to spiral helices is the basic assumption in the TGD based model of tornadoes. This suggests that Z^0 super-conductivity and, since rotating systems probably involve also magnetic fields, phenomena analogous to auroras could be involved also now.

It is indeed well known that luminous phenomena resembling those accompanying ball lightnings [47] are associated also with tornadoes [35, 36, 37]). Edward Lewis introduces the notion of plasmoid to explain a wide range of phenomena including ball lightnings and tornadoes. He assigns plasmons even with cold fusion (the damage resulting to Palladium target in cold fusion resembles the traces caused by ball lightnings, [28]) and super-conductivity (sic!). Although Lewis obviously over-generalizes the notion of plasmoid, one cannot deny that the concept has a strong theoretical appeal in it.

The findings of Lewis inspire some further ideas about the physics of many-sheeted space-time.

a) The runaway mechanism for ions from the magnetic flux tubes could provide a general mechanism behind luminous phenomena like auroras, lightnings, ball lightnings, sprites and tornadoes. Plasmoids would result when supra current becomes overcritical. The un-identified source of energy in these phenomena might be the energy associated with the supra currents.

b) The break-down of the super-conductivity could be understood in terms of a supra current leakage to non-super-conducting space-time sheets caused by the inertia of the current carriers. The critical temperature could be determined as the temperature below which the join along boundaries bonds between super-conducting and non-conducting space-time sheets are not formed. The temperature of super-conducting space-time sheets could be much more lower than this temperature but this is not necessary if high \hbar dark matter is in question.

c) The Trojan horse mechanism of cold fusion [F8] involves the notion many-sheeted space-time in an essential manner. Perhaps the supra currents running at the magnetic flux tube space-time sheets not containing the nuclear Coulombic fields provide the means to circumvent the Coulomb barrier.

References

[TGDview] M. Pitkänen (2006), *Topological Geometroynamics: Overview*.
<http://www.helsinki.fi/~matpitka/tgdview/tgdview.html>.

- [TGDgeom] M. Pitkänen (2006), *Quantum Physics as Infinite-Dimensional Geometry*.
<http://www.helsinki.fi/~matpitka/tgdgeom/tgdgeom.html>.
- [TGDquant] M. Pitkänen (2006), *Quantum TGD*.
<http://www.helsinki.fi/~matpitka/tgdquant/tgdquant.html>.
- [TGDclass] M. Pitkänen (2006), *Physics in Many-Sheeted Space-Time*.
<http://www.helsinki.fi/~matpitka/tgdclass/tgdclass.html>.
- [TGDnumber] M. Pitkänen (2006), *TGD as a Generalized Number Theory*.
<http://www.helsinki.fi/~matpitka/tgdnumber/tgdnumber.html>.
- [TGDpad] M. Pitkänen (2006), *p-Adic length Scale Hypothesis and Dark Matter Hierarchy*.
<http://www.helsinki.fi/~matpitka/paddark/paddark.html>.
- [TGDfree] M. Pitkänen (2006), *TGD and Fringe Physics*.
<http://www.helsinki.fi/~matpitka/freenergy/freenergy.html>.
- [TGDconsc] M. Pitkänen (2006), *TGD Inspired Theory of Consciousness*.
<http://www.helsinki.fi/~matpitka/tgdconsc/tgdconsc.html>.
- [TGDselforg] M. Pitkänen (2006), *Bio-Systems as Self-Organizing Quantum Systems*.
<http://www.helsinki.fi/~matpitka/bioselforg/bioselforg.html>.
- [TGDware] M. Pitkänen (2006), *Quantum Hardware of Living Matter*.
<http://www.helsinki.fi/~matpitka/bioware/bioware.html>.
- [TGDholo] M. Pitkänen (2006), *Bio-Systems as Conscious Holograms*.
<http://www.helsinki.fi/~matpitka/hologram/hologram.html>.
- [TGDgeme] M. Pitkänen (2006), *Mathematical Aspects of Consciousness Theory*.
<http://www.helsinki.fi/~matpitka/genememe/genememe.html>.
- [TGDdeeg] M. Pitkänen (2006), *TGD and EEG*.
<http://www.helsinki.fi/~matpitka/tgdeeg/tgdeeg/tgdeeg.html>.
- [TGDmagn] M. Pitkänen (2006), *Magnetospheric Consciousness*.
<http://www.helsinki.fi/~matpitka/magnconsc/magnconsc.html>.

- [TGDmath] M. Pitkänen (2006), *Mathematical Aspects of Consciousness Theory*.
<http://www.helsinki.fi/~matpitka/mathconsc/mathconsc.html>.
- [1] A. Schienle, R. Stark, R. Kulzer, R. Klpper and D. Vaitl (1996) *Atmospheric electromagnetism: individual differences in brain electrical response to simulated sferics*. International Journal of Psychophysiology, 21, 177.
- [2] R. O. Becker and G. Selden (1990) *The Body Electric: Electromagnetism and the Foundation of Life*. William Morrow & Company, Inc., New York.
- [3] G. Pollack (200?), *Cells, Gels and the Engines of Life*, Ebner and Sons.
<http://www.cellsandgels.com/> .
- [4] G. N. Ling (1962) *A physical theory of the living state: the association-induction hypothesis; with considerations of the mechanics involved in ionic specificity*. New York: Blaisdell Pub. Co..
Ibid(1978): *Maintenance of low sodium and high potassium levels in resting muscle cells*. Journal of Physiology (Cambridge), July: 105-23.
Ibid(1992): *A revolution in the physiology of the living cell*. Malabar, FL: Krieger Pub. Co..
- [5] G.N. Ling *et al*: *Experimental confirmation, from model studies, of a key prediction of the polarized multilayer theory of cell water*. Physiological Chemistry and Physics, 10:1, 1978: 87-8.
- [6] G. Ling, *Three sets of independent disproofs against the membrane-pump theory* <http://www.gilbertling.org/lp6a.htm> .
- [7] B. Sakmann and B. Neher (1983): *Single-channel recording*. Plenum Press, New York & London.
- [8] W. K. Purves and G. H. Orians (1987): *Life: The Science of Biology*. Sunderland, Massachusetts: Sinauer.
- [9] F. Sachs, F. Qin (1993), *Gated, ion-selective channels observed with patch pipettes in the absence of membranes: novel properties of a gigaseal*. Biophysical Journal, September: 1101-7.
- [10] A.A. Lev *et al* (1993), *Rapid switching of ion current in narrow pores: implications for biological ion channels*. Proceedings of the Royal Society of London. Series B: Biological Sciences, June, 187-92.

- [11] M. W. Ho (1993), *The Rainbow and the Worm*, World Scientific, Singapore.
Ibid (1994), *Coherent Energy, Liquid Crystallinity and Acupuncture*,
<http://www.consciousness.arizona.edu/quantum/Archives/Uploads/mifdex.cgi?msgindex.mif>.
- [12] M. W. Ho and P. T. Saunders(1994), *Liquid Crystalline Mesophase in living organisms*, in *Bioelectrodynamics and Biocommunication* (M. W. Ho, F. A. Popp and U. Warnke, eds), World Scientific, Singapore.
- [13] *Liquid crystals on line*, <http://www.lcionline.net/>
- [14] Fröhlich, H. (1975) *The extraordinary dielectric properties of biological materials and the action of enzymes*, Proc. Natl. Acad. Sci. 72:4211-4215.
- [15] W. Nagl, M. Rattemayer and F.A. Popp (1981), *Evidence of Photon Emission from DNA in Living Systems*, in *Naturwissenschaften*, Vol. 68, No 5, 577.
- [16] L. Milgrom (2001), *Thanks for the memory*. An article in Guardian about the work of professor M. Ennis of Queen's University Belfast supporting the observations of Dr. J. Benveniste about water memory. <http://www.guardian.co.uk/Archive/Article/0,4273,4152521,00.html>.
- [17] C. Smith (2001), *Learning From Water, A Possible Quantum Computing Medium*, talk in CASYS'2001, 5th international conference on Computing Anticipating Systems held in Liege, Belgium, August 13-18. Abstract book published by Chaos.
- [18] J. Benveniste *et al* (1988). *Human basophil degranulation triggered by very dilute antiserum against IgE*. Nature 333:816-818.
- [19] J. Benveniste *et al* (198?). *Transatlantic transfer of digitized antigen signal by telephone link*. Journal of Allergy and Clinical Immunology. 99:S175 (abs.). For recent work about digital biology and further references about the work of Benveniste and collaborators see <http://www.digibio.com/> .
- [20] B. E. W. Nordenström (1983): *Biologically Closed Electric Circuits*. Nordic Medical Publications, Arsenalsgatan 4, S-111 47 Stockholm, Sweden.

- [21] N. Cherry (2000), Conference report on effects of ELF fields on brain, <http://www.tassie.net.au/emfacts/icnirp.txt> .
- [22] D. J. Woodbury (1989): *Pure lipid vesicles can induce channel-like conductances in planar bilayers*. Journal of Membrane Biology, July 1989: 145-50.
- [23] M. Persinger (1999), "The tectonic strain theory as an explanation for UFO phenomena", <http://www.laurentian.ca/www/neurosci/tectonicedit.htm>.
Ibid (1995), "On the possibility of directly accessing every human brain by electromagnetic induction of fundamental algorithms", Percept. Mot. Skills, 80(3 Pt 1), 791-9.
Ibid (1987), *Neuropsychological Bases of God Beliefs*, Praeger Publishers.
- [24] Luca Gammaitoni *et al* (1998) *Stochastic Resonance*, Rev. Mod. Phys. 70, 223-288, January. <http://www.umbrars.com/sr/> .
- [25] D. J. E. Callaway (1992) *Landau, Abrikosov, Hofstadter: Magnetic Flux Penetration in a Lattice Super-conductor*, Ann. of Phys. 224, 210 (1993).
- [26] S. W. Kuffler, J. S. Nicholis and A. R. Martin (1984), *From Neuron to Brain*, Sinauer Associates Inc. Publishers, Sutherland, Massachusetts.
- [27] K. Abe *et al* (1994), Phys. Rev. Lett. Vol 73, No 1.
- [28] E. Lewis (1994), *Plasmoids and Cold Fusion*, Cold Fusion Times, 2, no. 1, 4 (Summer).
- [29] T. L. Hansen (2001), *The northern lights-what are they?*, <http://geo.phys.uit.no/articl/theaurora.html> .
- [30] G. Zgrablic *et al*(2001), *Instrumental recording of electrophonic sounds from Leonid fireballs*. To be published in Journal of Geophysical Research. <http://fizika.org/ilwcro/results/> . See also news release in same URL address.
- [31] B. U. O. Sonnerup (1979), in Solar System Plasma Physics, vol. III, L. T. Lanzerotti, C. F. Kennel, E. N. Parker, eds., North-Holland, New York, p.45.
- [32] M. Oieroset, T. D. Phan, M. Fujimoto, R. P. Lin, R. P. Lepping (2001), Nature 412, 414.

- [33] G. T. Marklund *et al* (2001), *Nature* vol. 414, 13, December., p.724, <http://www.nature.com> .
- [34] C. Day (2001), *Spacecraft Probes the Site of Magnetic Reconnection in Earth's Magnetotail*, *Physics to Day* vol 54 iss. 10 p. 16. <http://www.physicstoday.org/pt/vol-54/iss-10/p16.html> .
- [35] E. Lewis (1994), *Luminous Tornadoes and Other Plasmoids*, *Cold Fusion Times*, 1 (no. 4), 4 (Winter).
- [36] M. Brook, "Electric Currents Accompanying Tornado Activity," *Science*, 157, 1434 (Sept. 22, 1967).
- [37] B. Vonnegut and J. Weyer(1966) , *Luminous Phenomena in Nocturnal Tornadoes*, *Science*, 153, 1213 (Sept. 9).
- [38] Wisconsin University (2003), *Twister: The Tornado Story*, <http://whyfiles.org/013tornado/3.html>.
- [39] E. Lozneau and M. Sanduloviciu (2003) *Minimal-cell system created in laboratory by self-organization*, *Chaos, Solitons & Fractals*, Volume 18, Issue 2, October, p. 335.
See also *Plasma blobs hint at new form of life*, *New Scientist* vol. 179 issue 2413 - 20 September 2003, page 16.
- [40] E. A. Bering (1983), *Apparent electrostatic ion cyclotron waves in the diffuse aurora*, *Geophysical Research Letters*, vol. 10, Aug. p. 647-650. <http://www.agu.org/journals/gl/>.
- [41] University of California (1999), *Auroras, Paintings in the Sky*, http://www.exploratorium.edu/learning_studio/auroras/happen.html.
- [42] Roshchin, V.V and Godin, S.M., *An Experimental Investigation of the Physical Effects in a Dynamic Magnetic System*, *New Energy Technologies Issue #1 July-August 2001*.
- [43] D. D. Sentman, E. M. Wescott (1993), *Geophys. Res. Lett.* 20. 2857.
- [44] W. A. Lyons (1994), *Geophys. Res. Lett.* 21, 875.
- [45] C. T. R. Wilson (1925), *Proc. Phys. Soc. London* 37, 32D.
- [46] E. R. Williams (2001), *Sprites, Elves, and Glow Discharge Tubes*, feature article of *Physics to Day*, vol. 52, No 11.

- [47] G. Egely (1988), *Physical Problems and Physical Properties of Ball Lightning*, Proc. First International Symposium on Ball Lightning (Fire ball) – The Science of Ball Lightning (Fire Ball) Tokyo, Japan, July 4-6, World Scientific Company, Singapore.
- [48] *Lightning*, Wikipedia article,
<http://en.wikipedia.org/wiki/Lightning>.
- [A1] The chapter *An Overview about the Evolution of Quantum TGD* of [TGDview].
<http://www.helsinki.fi/~matpitka/tgdview/tgdview.html#tgdevo>.
- [C12]
- [C6] The chapter *Was von Neumann Right After All* of [TGDquant].
<http://www.helsinki.fi/~matpitka/tgdquant/tgdquant.html#vNeumann>.
- [D6] The chapter *TGD and Astrophysics* of [TGDclass].
<http://www.helsinki.fi/~matpitka/tgdclass/tgdclass.html#astro>.
- [D7] The chapter *Macroscopic Quantum Phenomena and CP_2 Geometry* of [TGDclass].
<http://www.helsinki.fi/~matpitka/tgdclass/tgdclass.html#super>.
- [D7] The chapter *Macroscopic Quantum Phenomena and CP_2 Geometry* of [TGDclass].
<http://www.helsinki.fi/~matpitka/tgdclass/tgdclass.html#super>.
- [E9] The chapter *Topological Quantum Computation in TGD Universe* of [TGDnumber].
<http://www.helsinki.fi/~matpitka/tgdnumber/tgdnumber.html#tqc>.
- [F3] The chapter *p-Adic Particle Massivation: Hadron Masses* of [TGDpad].
<http://www.helsinki.fi/~matpitka/paddark/paddark.html#padmass2>.
- [F4] The chapter *p-Adic Particle Massivation: Hadron Masses* of [TGDpad].
<http://www.helsinki.fi/~matpitka/paddark/paddark.html#padmass3>.
- [F6] The chapter *Topological Condensation and Evaporation* of [TGDpad].
<http://www.helsinki.fi/~matpitka/paddark/paddark.html#padaelem>.
- [F7] The chapter *The Recent Status of Leptohadron Hypothesis* of [TGDpad].
<http://www.helsinki.fi/~matpitka/paddark/paddark.html#leptc>.

- [F8] The chapter *TGD and Nuclear Physics* of [TGDpad].
<http://www.helsinki.fi/~matpitka/paddark/paddark.html#padnucl>.
- [F9] The chapter *Dark Nuclear Physics and Living Matter* of [TGDpad].
<http://www.helsinki.fi/~matpitka/paddark/paddark.html#exonuclear>.
- [G2] The chapter *The Notion of Free Energy and Many-Sheeted Space-Time Concept* of [TGDfree].
<http://www.helsinki.fi/~matpitka/freenergy/freenergy.html#freenergy>.
- [G3] The chapter *Did Tesla Discover the Mechanism Changing the Arrow of Time?* of [TGDfree].
<http://www.helsinki.fi/~matpitka/freenergy/freenergy.html#tesla>.
- [H1] The chapter *Matter, Mind, Quantum* of [TGDconsc].
<http://www.helsinki.fi/~matpitka/tgdconsc/tgdconsc.html#conscic>.
- [H3] The chapter *Self and Binding* of [TGDconsc].
<http://www.helsinki.fi/~matpitka/tgdconsc/tgdconsc.html#selfbindc>.
- [H7] The chapter *Conscious Information and Intelligence* of [TGDconsc].
<http://www.helsinki.fi/~matpitka/tgdconsc/tgdconsc.html#intsysc>.
- [I1] The chapter *Quantum Theory of Self-Organization* of [TGDselforg].
<http://www.helsinki.fi/~matpitka/bioselforg/bioselforg.html#selforgac>.
- [I3] The chapter *Biological Realization of Self Hierarchy* of [TGDselforg].
<http://www.helsinki.fi/~matpitka/bioselforg/bioselforg.html#bioselfc>.
- [I4] The chapter *Quantum Control and Coordination in Bio-systems: Part I* of [TGDselforg].
<http://www.helsinki.fi/~matpitka/bioselforg/bioselforg.html#qcococI>.
- [I5] The chapter *Quantum Control and Coordination in Bio-Systems: Part II* of [TGDselforg].
<http://www.helsinki.fi/~matpitka/bioselforg/bioselforg.html#qcococII>.
- [J1] The chapter *Bio-Systems as Super-Conductors: part I* of [TGDware].
<http://www.helsinki.fi/~matpitka/bioware/bioware.html#superc1>.
- [J2] The chapter *Bio-Systems as Super-Conductors: part II* of [TGDware].
<http://www.helsinki.fi/~matpitka/bioware/bioware.html#superc2>.
- [J4] The chapter *Quantum Antenna Hypothesis* of [TGDware].
<http://www.helsinki.fi/~matpitka/bioware/bioware.html#tubuc>.

- [J5] The chapter *Wormhole Magnetic Fields* of [TGDware].
<http://www.helsinki.fi/~matpitka/bioware/bioware.html#wormc>.
- [J6] The chapter *Coherent Dark Matter and Bio-Systems as Macroscopic Quantum Systems* of [TGDware].
<http://www.helsinki.fi/~matpitka/bioware/bioware.html#darkbio>.
- [K1] The chapter *Time, Spacetime and Consciousness* of [TGDholo].
<http://www.helsinki.fi/~matpitka/hologram/hologram.html#time>.
- [K3] The chapter *General Theory of Qualia* of [TGDholo].
<http://www.helsinki.fi/~matpitka/hologram/hologram.html#qualia>.
- [K4] The chapter *Bio-Systems as Conscious Holograms* of [TGDholo].
<http://www.helsinki.fi/~matpitka/hologram/hologram.html#hologram>.
- [K5] The chapter *Homeopathy in Many-Sheeted Space-Time* of [TGDholo].
<http://www.helsinki.fi/~matpitka/hologram/hologram.html#homeoc>.
- [K6] The chapter *Macroscopic Quantum Coherence and Quantum Metabolism as Different Sides of the Same Coin* of [TGDholo].
<http://www.helsinki.fi/~matpitka/hologram/hologram.html#metab>.
- [L1] The chapter *Genes and Memes* of [TGDgame].
<http://www.helsinki.fi/~matpitka/genememe/genememe.html#genememec>.
- [L2] The chapter *Many-Sheeted DNA* of [TGDgame].
<http://www.helsinki.fi/~matpitka/genememe/genememe.html#genecodec>.
- [L4] The chapter *Pre-Biotic Evolution in Many-Sheeted Space-Time* of [TGDgame].
<http://www.helsinki.fi/~matpitka/genememe/genememe.html#prebio>.
- [M1] The chapter *Magnetic Sensory Canvas Hypothesis* of [TGDeeg].
<http://www.helsinki.fi/~matpitka/tgdeeg/tgdeeg/tgdeeg.html#mec>.
- [M2] The chapter *Quantum Model for Nerve Pulse* of [TGDeeg].
<http://www.helsinki.fi/~matpitka/tgdeeg/tgdeeg/tgdeeg.html#pulse>.
- [M3] The chapter *Dark Matter Hierarchy and Hierarchy of EEGs* of [TGDeeg].
<http://www.helsinki.fi/~matpitka/tgdeeg/tgdeeg/tgdeeg.html#eegdark>.
- [M4] The chapter *Quantum Model for EEG: Part I* of [TGDeeg].
<http://www.helsinki.fi/~matpitka/tgdeeg/tgdeeg/tgdeeg.html#eegI>.

- [M6] The chapter *Quantum Model for Hearing* of [TGDeeg].
<http://www.helsinki.fi/~matpitka/tgdeeg/tgdeeg/tgdeeg.html#hearing>.
- [N1] The chapter *Magnetospheric Sensory Representations* of [TGDmagn].
<http://www.helsinki.fi/~matpitka/magnconsc/magnconsc.html#srepres>.

4

OCULAR DOMINANCE COLUMNS IN MONKEY CORTEX demonstrated by injection of radioactive proline into one eye. (A) and (B) are autoradiographs photographed with dark field illumination in which the silver grains appear white. (A) This horizontal section first passes through the visual cortex at right angles to the surface displaying columns cut perpendicularly, then in the center horizontally through layer IV cutting columns tangentially. (B) Reconstruction made from numerous horizontal sections of layer IVC in another monkey in which the ipsilateral eye had been injected (no single horizontal section can encompass more than a part of layer IV of the cortex because of its curvature). Dorsal is above, medial to the right. In both (A) and (B), the ocular dominance columns appear as stripes of equal width supplied by one eye or the other. (C) Reconstruction of the pattern of ocular dominance columns over the entire exposed part of layer IVC. Scale 5 mm. (A and B from LeVay, unpublished, photos by courtesy of S. LeVay; C from LeVay, Hubel, and Wiesel, 1975.)

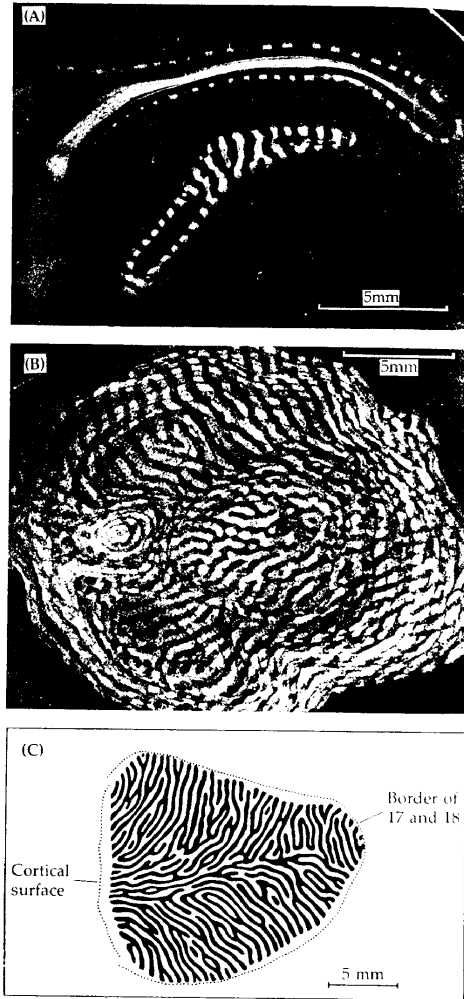
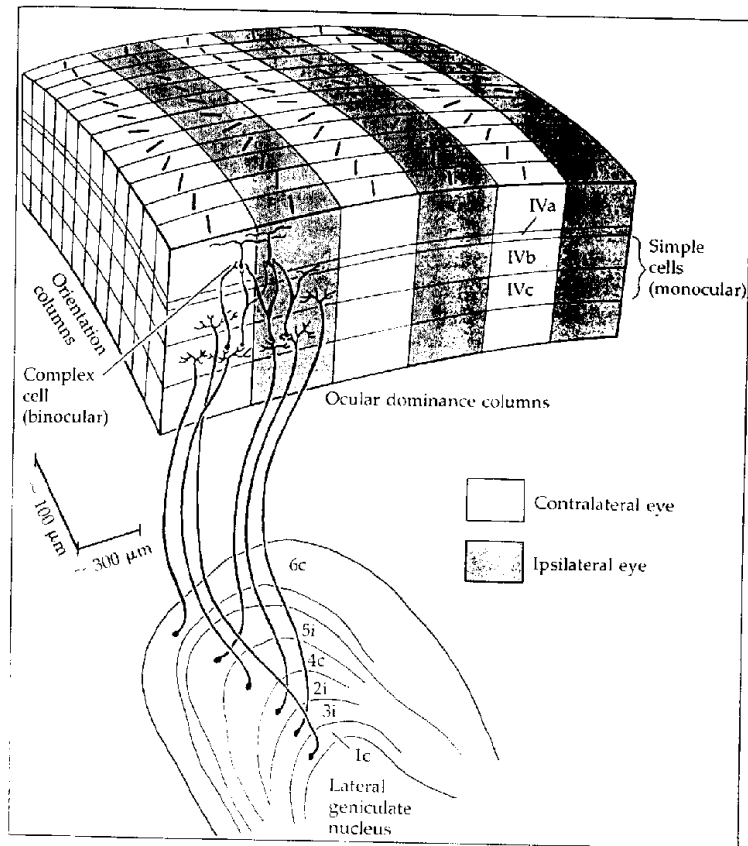


Figure 1:



7 RELATION BETWEEN OCULAR DOMINANCE and orientation columns. Scheme in which the ocular dominance and orientation columns run at right angles to each other. An example of a complex cell is shown in an upper layer, receiving its inputs from two simple cells that lie in adjacent ocular dominance columns but share the same orientation columns. (From Hubel and Wiesel, 1972.)

Figure 2: